Journal Pre-proof

Recent Progress in Developing Li₂S Cathodes for Li-S Batteries

Shiqi Li ^a, Dan Leng ^a, Wenyue Li ^b, Long Qie ^c, Zhihua Dong ^a, Zhiqun Cheng ^a, Zhaoyang Fan ^{b, *}

^a College of Electronic Information, Hangzhou Dianzi University, Hangzhou, 310018, China.

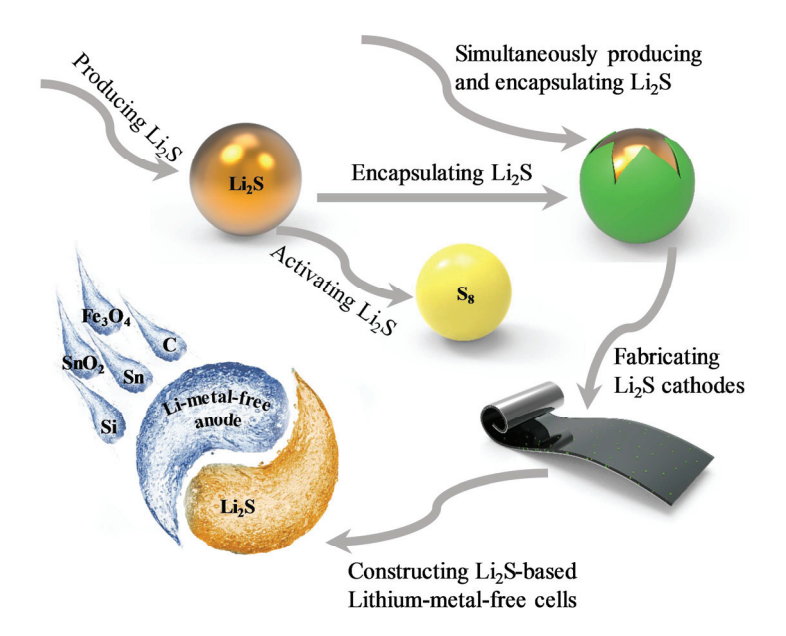
^b Department of Electrical and Computer Engineering and Nano Tech Center, Texas Tech University, Lubbock, Texas 79409, USA.

^c Institute of New Energy Vehicles, School of Materials Science & Engineering, Tongji University, Shanghai, 200092, China.

* Corresponding author.

E-mail addresses: zhaoyang.fan@ttu.edu (Z. Fan).

Graphical abstract



Recent Progress in Developing Li₂S Cathodes for Li-S Batteries

Abstract

With its unique features, lithium sulfide (Li₂S) has been investigated as the cathode material for next-generation rechargeable batteries. Even though Li₂S itself cannot solve all the problems faced by lithium-sulfur batteries (LSBs) and it may also introduce new issues, it does provide new opportunities. As the fully lithiated state of sulfur, Li₂S offers the prospect of lithium-metal-free anodes and will also alleviate the volume expansion issues otherwise occurred in the sulfur cathode. Perhaps a most radical change when substituting sulfur with Li₂S lies at the high-temperature process ability of the latter, thus opening new avenues to construct rationally designed electrodes. Despite sharing certain similarities with sulfur-based LSB, Li₂S-based has its own opportunities and challenges in term of material synthesis, electrode fabrication, cell construction, and electrochemical behavior. To advance its state of the art, this review article discusses the current understandings on the initial Li₂S activation process, which plays a crucial role in guiding Li₂S nanostructure design and fabrication. With this leading thread, the article surveys impactful works on producing Li₂S nanoparticles, encapsulating Li₂S nanoparticles, simultaneously producing and encapsulating Li₂S nanoparticles, and fabricating Li₂S cathodes, followed by constructing lithium-metal-free LSBs. The pros and cons of different methods and the associated electrochemical behaviors are highlighted. Throughout, we call out the important research opportunities and challenges, both scattered out in the survey and aggregated in our conclusion perspective on future works, towards the fundamental understanding and practical development of Li₂S-based LSBs.

1. Introduction

Lithium-sulfur batteries (LSBs), by pairing a sulfur cathode with a lithium-metal anode, offer a high theoretical energy density of 2600 Wh Kg⁻¹ when sulfur is fully converted into lithium sulfide (Li₂S). As an electrode material, sulfur also possesses other merits such as low cost, resource abundance, and environmental benignity. As such, LSBs has been under intensive development as one of the most promising next-generation rechargeable batteries used for electrified transportation and stationary energy storage, among others.¹⁻³

Despite the tremendous potential and decades of hard endeavor, the LSB technology is still immature. The extremely insulative nature of sulfur and Li₂S, both electronically and ionically, makes a solid-solid reaction kinetically very challenging, if ever surmountable. Even worse, although the soluble characteristic of intermediate lithium polysulfides (Li₂S_x, 4 $\leq x \leq 8$) in ether-based electrolytes can be leveraged to relieve the otherwise formidable reaction kinetic barrier, shuttling of these same polysulfides between the cathode and the anode results in a series of adverse consequences, another perhaps more intractable challenge. In addition, the common electrode issues, such as a large volume change also exist in the sulfur cathode with ~ 80 % expansion during sulfur discharge.⁴⁻⁷ These problems give rise to low specific capacity, low rate capability, low Coulombic efficiency, and poor cycling stability for most reported LSB cells. Pairing with lithium-metal anodes will inevitably pose great safety issues due to the formation of lithium dendrites during the charging and discharging process, and the polysulfide shuttling will only make things worse. The chemical reactions of lithium metal with the electrolyte and Li_2S_x and the repeated solid electrolyte interface (SEI) formation and destruction cause significant loss of active materials and electrolytes. In many reports on LSBs that claimed a high energy density and long cycling stability, much excessive electrolyte and Li anode mass were used, resulting in an extremely low practical energy density when all the masses are counted.⁸

Instead of elemental sulfur, Li₂S, the fully lithiated state of sulfur, is attractive as an alternative cathode material. Using Li₂S as the starting material could circumvent the volume expansion issue and the resulted cathode pulverization. Additionally, with Li₂S as the cathode, graphite, Si, Sn and others could be used as a lithium-free anode, ⁹⁻¹² and thereby avoiding the safety issues of the metallic lithium anode.

Since the battery chemistry is still based on the conversion between Li₂S and S, using Li₂S as the starting material does not solve other challenging problems such as poor electronic and ionic conductivities of the active materials as well as the polysulfides shuttle effects. ^{13, 14} Similar to the case of sulfur, blending or encapsulating Li₂S with electronically or ionically conductive matrix is still necessary, which also help alleviate shuttle effects of Li₂S_x. ¹⁵⁻¹⁸ In this regard, Li₂S again is superior to sulfur because this encapsulation process could be carried out at a much higher temperature due to its high melting point (938 °C), while for sulfur, this temperature is limited to below 200 °C by its high vapor pressure. Thus, many preparation strategies for forming ideal composites that cannot be applied for sulfur now become viable for Li₂S. ¹⁹⁻²¹

However, using Li₂S as the starting cathode material introduces its own issues. The Li₂S activation in the first charging process turns out to be a formidable problem since it requires an extraordinary overpotential if the cathode structure is not properly designed.²² This overpotential is directly related to the particle size, morphology, and crystallinity of used Li₂S.

The commercially available Li₂S,²³⁻²⁷ with a particle size of tens of micrometers and hence very poor electrochemical property, is not a suitable candidate. Furthermore, Li₂S is reactive to humidity, and the conventional slurry-casting process to prepare cathodes must be modified to prevent Li₂S from exposing to ambient atmosphere. All these new problems introduced by Li₂S itself demand rational design and preparation of Li₂S composites and cathode structures in order to achieve high-performance and cost-effective LSBs.

In the literature, comprehensive reviews on LSBs, particularly those based on sulfur cathodes, have been well published, ²⁸⁻⁴⁵ while articles reviewing works exclusively on Li₂S cathodes are quite few. 46-49 Considering the dramatic differences in the physical and chemical properties between sulfur and Li₂S, different strategies and approaches to prepare the active material and the cathode structure are needed. With growing interest in Li₂S as the initial active material and particularly dramatic progress in recent years, it becomes necessary to review the status in this area and provide tutorial and guidance to new investigators. Toward this end, this review article starts section 2 by introducing the most challenging issue of Li₂S material activation and recapitulates the three main strategies for reducing the activation voltage. Once the activation process is completed with Li₂S fully converted to elemental sulfur, the Li₂S-based cathode will behave similarly as the sulfur-based cathode.⁵⁰ Therefore, similar electrode design practices applied to the sulfur cathode will also be applied to the Li₂S cathode. These includes incorporation of host materials to enhance the electronic and ionic conductivities of the whole cathode, physically confine and chemically bond the soluble polysulfides to minimize their diffusion out of the cathode structure, catalyze the redox reaction to accelerate the charge-transfer rate, etc. Therefore, in conjunction with Li₂S

activation articulated in section 2, Section 3 reviews the different methods in producing Li₂S nanoparticles, Section 4 covers Li₂S nanoparticle encapsulation, and Section 5 focuses on strategies of simultaneously producing and encapsulating Li₂S nanoparticles. After emphasizing these different aspects, Section 6 gives a summary on how to fabricate a high-quality Li₂S cathode. Finally, Section 7 considers electrolytes and lithium-metal-free anodes to construct high-performance Li₂S batteries. Throughout each section, we call out challenges and research opportunities, which are further captured in the concluded summary in section 8, where our perspectives on future works are especially emphasized towards developing practical Li₂S-based LSB technology in a near future. This review is organized following the logic structure as illustrated in Fig. 1.

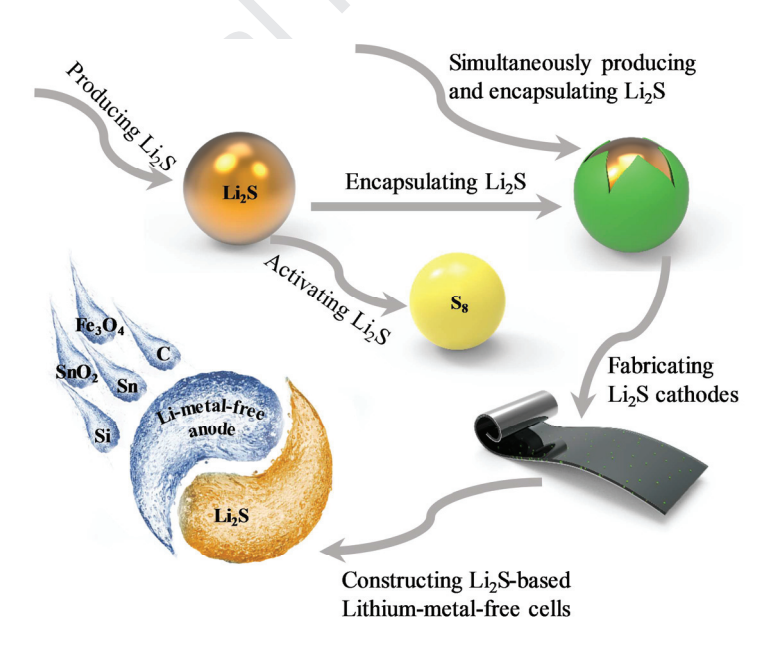


Fig. 1. Schematic illustrating the logic structure of this review.

2. Li₂S activation

2.1 The large activation barrier

The commercially available Li₂S particles have a random size distribution from several micrometers to tens of micrometers.^{22, 51} When this microscale Li₂S powder is directly applied to prepare the cathode, a large potential barrier more than 1.0 V will appear in the first charge cycle. Fig. 2 (a) shows a typical initial charging curve. 22, 52 The large barrier limits the charging depth causing low utilization of the active material. The existence of both the long plateau and the barrier implies that the initial charging process is a two-phase reaction, and this barrier is related to phase nucleation, for which an extra driving force is required.²² To reveal factors contributing to the barrier, Yang et al. investigated the relation between charging rates and barrier heights, as shown in Fig. 2 (b, c). 22 The barrier height is nearly a constant (as small as ~ 25 mV) at low current rates (C/2000 - C/500) where thermodynamics dominate. This value is negligible compared with that (0.5 - 1 V) at moderate rates. At high current rates (> C/200), the barrier height linearly increases with the logarithm of the current rate and thus kinetic factors come into play. 22 Therefore, at practical rates, the kinetic factors rather than the thermodynamics determine this barrier height. Further investigations, particularly those based on the Butler-Volmer model, reveal that among the three kinetic factors, electronic conductivity of Li₂S, diffusivity of the Li⁺ in Li₂S, and charge transfer at the surface of Li₂S, the latter two especially the charger transfer process dominate the barrier height while the effect of low electronic conductivity is trivial.²² For instance, the charge transfer process is much faster between Li₂S and polysulfides than that between Li₂S and an electrolyte without polysulfides, which was validated by electrochemical impedance spectrum (EIS) measurement,²² and thus the initial charging barrier dramatically reduced or even disappeared when lithium polysulfides were applied as additives to the electrolytes.²² This reasoning can also explain two other observations that no obvious initial charging barrier exists for sulfur-based LSBs, and the barrier disappears after the initial charging of Li₂S-based cathodes. After initial discharging of sulfur-based or Li₂S-based cathodes, lithium polysulfides appear in the electrolyte, which promote the charge transfer between Li₂S and the electrolyte.^{22, 53}

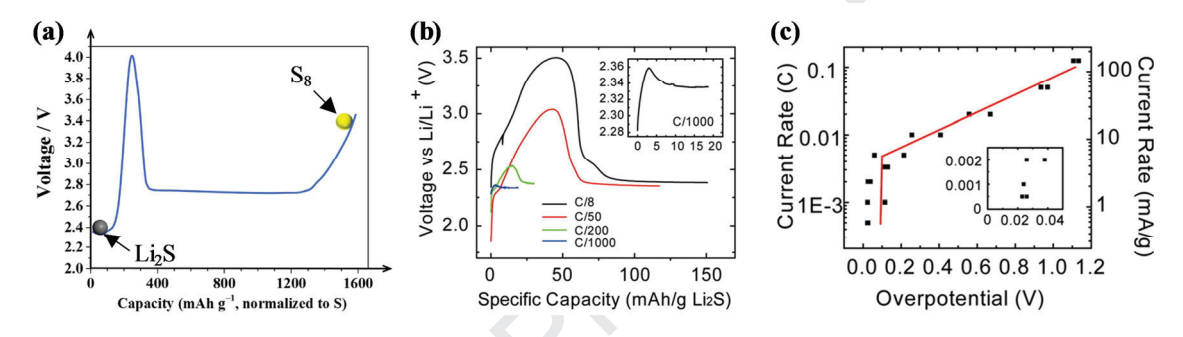


Fig. 2. (a) A typical initial charging curve of Li_2S cathodes.⁵² Reproduced with permission from Nature Publishing Group. (b) The initial charging barriers at different rates (1 C = 1166 mA g⁻¹) and (c) Relation between the current rate and the charging barrier.²² Reproduced with permission from American Chemical Society.

The origin of this charging barrier has been known, but the community has no consensus on the detailed charging processes. At least three different views have been proposed to expound the activation process of Li₂S in the initial charging process. As illustrated in Fig. 3 (a),^{54, 55} some authors suggest that a portion of Li₂S is directly transformed to sulfur (reaction I) that will partly dissolve in the electrolyte (reaction II) and then react with Li₂S to form long-chain lithium polysulfides (reaction III). Since the liquid to solid conversion is more favorable than solid to solid conversion, long-chain lithium polysulfides will be quickly

oxidized to sulfur (reaction IV). Thereby, the appearance of lithium polysulfides during the first charging process is mainly determined by the amount of sulfur dissolved in the solvent. Other investigators^{22, 56, 57} consider that, as in Fig. 3 (b), the activation process involves the electrochemical oxidization of surficial Li₂S first to short-chain Li₂S_x and then to long-chain Li₂S_x, after which the huge potential barrier will disappear. This is because the dissolved long-chain Li_2S_x can directly oxidize solid Li_2S . The third opinion⁵³ considers that during the initial charging process, Li₂S is directly converted to elemental sulfur through a two-phase transformation with a large overpotential to extract Li⁺ from the ionic bonded Li₂S into the electrolyte. As shown in Fig. 3 (c), the presence of an isosbestic point in the stack plot of X-ray absorption spectroscopy (XAS) spectra at different charge stages suggests a dominating two-phase transformation in the initial charging process. However, Li₂S is oxidized first to lithium polysulfides and then to sulfur in the second charging process through both electrochemical and chemical reactions. The difference between the first two charging processes comes from the residual lithium polysulfides after the first discharging process, which not only chemically react with Li₂S and act as the polysulfide facilitator for the electrochemical oxidation of Li₂S, but also facilitate the charge transfer at the Li₂S/electrolyte interface. It should be mentioned that other interpretations on the activation process have also been put forward.^{58, 59} These different opinions on how Li₂S is activated in the initial charging process might be related to the different Li₂S cathode structures studied and the different characterization tools used, since different tools might capture different features in a complex reaction process.

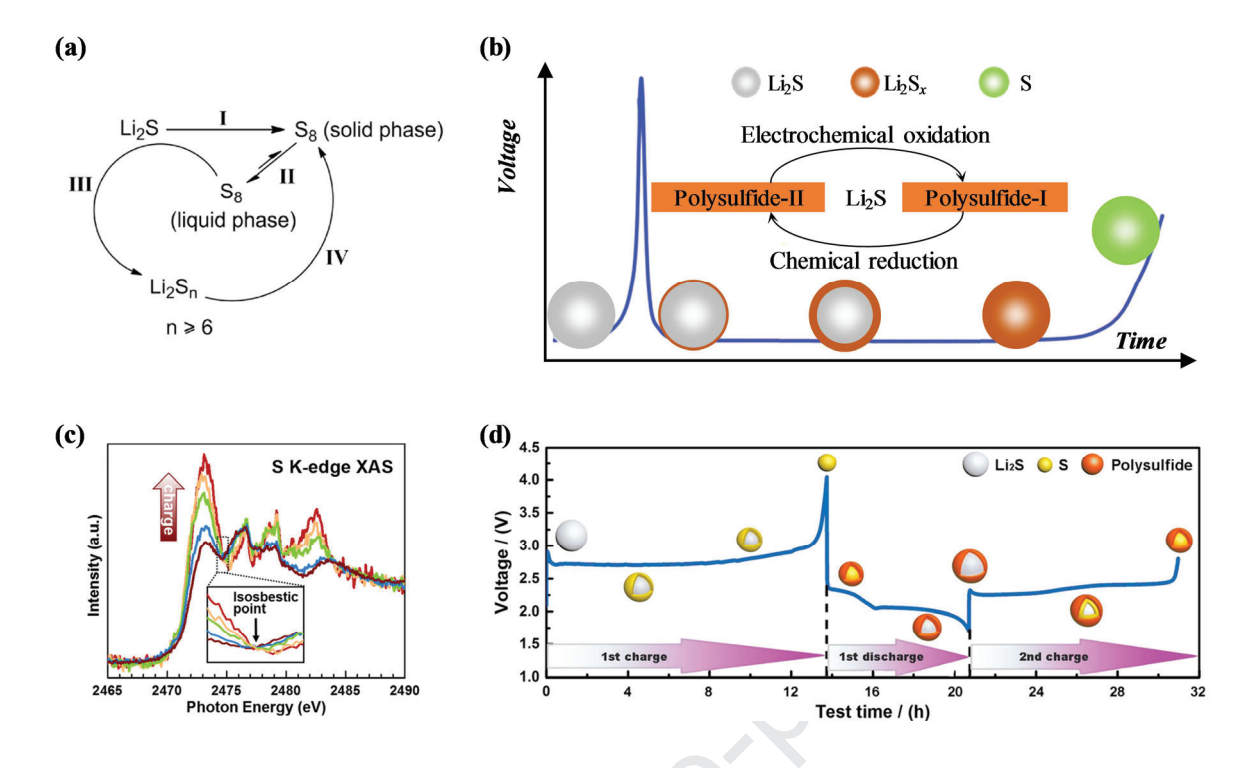


Fig. 3. Schematic illustrations of different interpretations on the Li₂S activation process in the first charging process. (a) Proposed by Vizintin et al.⁵⁴ Reproduced with permission from Elsevier. (b) Proposed by Wang et al.⁵⁶ Reproduced with permission from Royal Society of Chemistry. (c) XAS spectra during the charging process.⁵³ The insert shows the presence of an isosbestic point. Reproduced with permission from American Chemical Society. (d) Proposed by Zhang et al. ⁵³ Reproduced with permission from American Chemical Society.

2.2 Reducing the activation barrier

In a rechargeable battery, the initial activation process usually plays a crucial role in determining the battery performance since side reactions in this initial activation process, if not properly controlled, could irreversibly consume considerable amount of active electrode materials and/or electrolytes. Although microscale Li₂S particles could be activated using a

high cutoff voltage (~ 4 V vs. Li/Li⁺), such a high potential would lead to the decomposition of the commonly used ether-based electrolyte and the corrosion of the Al current collector in bis(trifluoromethane)sulfonimide lithium (LiTFSI)-contained electrolyte, thus degrading the LSB performance rapidly.^{60, 61} Three strategies, modifying the electrolytes by additives, engineering the Li₂S particles, and developing host materials as an activation facilitator, have been investigated to reduce the activation potential of Li₂S powder.

2.2.1 Modifying the electrolytes

Ammonium, ethanol, or lithium iodide (LiI) was applied as additives to enhance the dissolution of Li₂S in the electrolyte, thereby increasing the contact area of Li₂S with both the conductive carbon materials and the electrolyte. This will assist realization of fast reaction kinetics of Li₂S with great alleviation of initial large activation voltage.⁶²⁻⁶⁴

Adding P_2S_5 into the electrolyte helps form sulfur- and phosphorus-containing species on the surface of Li_2S . They can enhance charge transfer between Li_2S particles and electrolytes, and thus promoting Li_2S oxidation.⁶⁵

Perhaps the concept of introducing redox mediators (RMs) in the electrolyte is more intriguing. This idea has been widely applied in lithium-oxygen batteries to reduce the charge overpotential of Li₂O₂ for improving the energy efficiency and cycling stability of lithium-oxygen batteries. The application of RMs to reduce Li₂S charge overpotential has just started attracting interest. Their function can be captured as that during the charge process, the oxidized RMs in the electrolyte with a redox potential higher than that of Li₂S chemically oxidize Li₂S over its entire surface contacting with the electrolyte, and these reduced RMs then diffuse to the current collector where they are electrochemically

Journal Pre-proof

re-oxidized (Fig. 4 (a)).⁶⁹ Tsao et al. proposed three criteria for developing RMs that can expedite Li₂S oxidation.⁶⁹ The redox potential of RMs should be slightly higher than the equilibrium potential of Li₂S (around 2.15 V versus Li⁺/Li) to minimize the hysteresis between charging and discharging for a high energy efficiency. The RMs should also have high solubility and cycling stability in the electrolyte. Based on these criteria, the RM (1,5-bis(2-(2-(2-methoxyethoxy)ethoxy)ethoxy) anthra-9,10-quinone, abbreviated as AQT) was recently developed that reduced the activation voltage of Li₂S microparticles to 2.45 V from 3.6 V.⁶⁹ This progress makes it very promising to directly apply the commercial microscale Li₂S particles for Li₂S electrode fabrication. Other RMs including lithium polysulfides,^{22, 70-73} perylene bisimide,⁷⁴ Fe(η₅-C₅Me₅)₂,⁷⁵ and InI₃ have also been tested to reduce the activation potential of Li₂S.⁷⁶

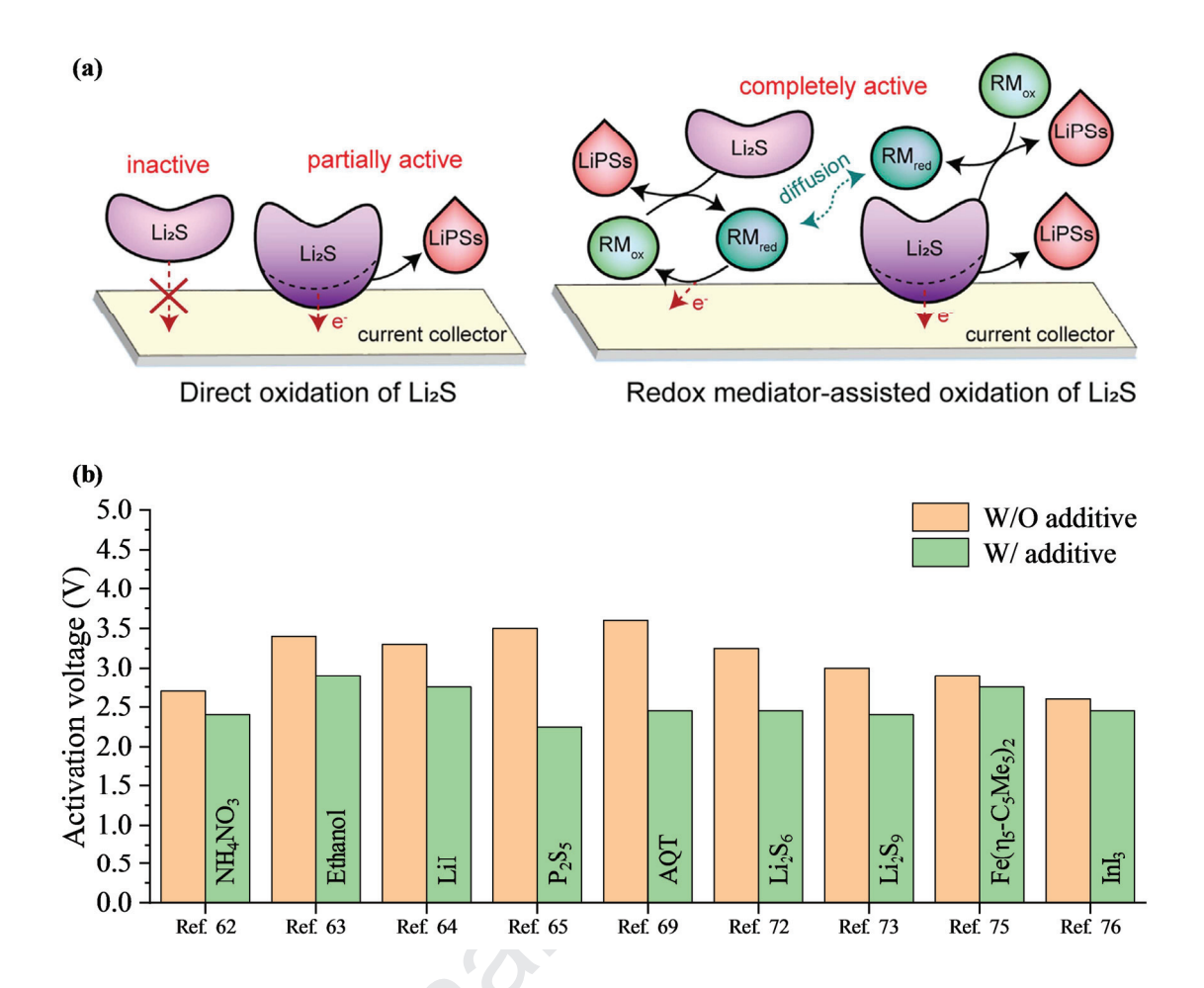


Fig. 4. (a) A schematic illustrating the direct Li₂S oxidation and the RM-assisted Li₂S oxidation in LSBs.⁶⁹ Reproduced with permission from Cell press. (b) Effects on reducing the activation voltage of Li₂S by adding different additives.

The reported reduction of activation voltage by several electrolyte additives is summarized in Fig. 4 (b), indicating their effectiveness in this regard. More studies and particularly calculation-guided RM design and test are needed to fully exploit their potentials. Incorporating the additive in the electrolyte is a facile step, making its industrial scalability feasible. Nevertheless, the adverse effects of certain additives on the anode and other electrochemical performance should be thoroughly investigated.

2.2.2 Engineering Li₂S particles

Since Li₂S activation is restricted by its low ionic conductivities, reducing the particle size to nanoscale is a natural approach for facilitating its activation. As shown in Fig. 5 (a), the microscale Li₂S powder based composites exhibit a charge barrier higher than 0.5 V, while those of nanoscale Li₂S exhibit a trivial potential barrier during the initial charging process, indicating the crucial role of particle size in its electrochemical kinetics. 77 As noticed from the cyclic voltammetry (CV) measurement, a voltage cutoff higher than 3.4 V is needed to activate the microscale particles, while it is only 2.45 V for the nanoscale ones. This further indicates the superior reaction kinetics for Li₂S at the nanoscale.⁷⁸ The enlarged surface area resulting from the reduced particle size would promote the lithium exchange rate at the interface between Li₂S particle and the electrolyte. The much easier activation of nanoscale Li₂S particle than its microscale counterpart is also reflected by studies of their EIS and ionic conductivity. As shown in Fig. 5 (b), the EIS of Li₂S nanoparticle-based electrode exhibits smaller semicircle and larger slope than that of microscale particle-based, indicating faster charge transfer and faster lithium-ion diffusion for the former than the latter. 78 Lin et al. found that compared to Li₂S microscale particles, the ionic conductivity of nanoscale ones could be increased by two orders of magnitude (Fig. 5 (c)),⁷⁹ further confirming the advantages of Li₂S nanoparticles. When the diameter of Li₂S particles was decreased to sub-nanometer such as Li₂₀S₁₀ cluster, the overpotential becomes only 0.37 V for delithiation, as revealed by the ab initio calculation.⁵⁷ Nevertheless, such small Li₂S atomic clusters have not been experimentally achieved yet.

As for the Li₂S cathode with non-uniform particle sizes, the smaller particles are preferentially electrochemically oxidized first, and the generated dissolved lithium polysulfides act as the redox mediators to promote the oxidation of larger particles whose dissolution rate is significantly suppressed at a low potential due to their small specific surface area. This observation agrees well with that a small amount of Li_2S_x added in the electrolyte can facilitate Li_2S activation.

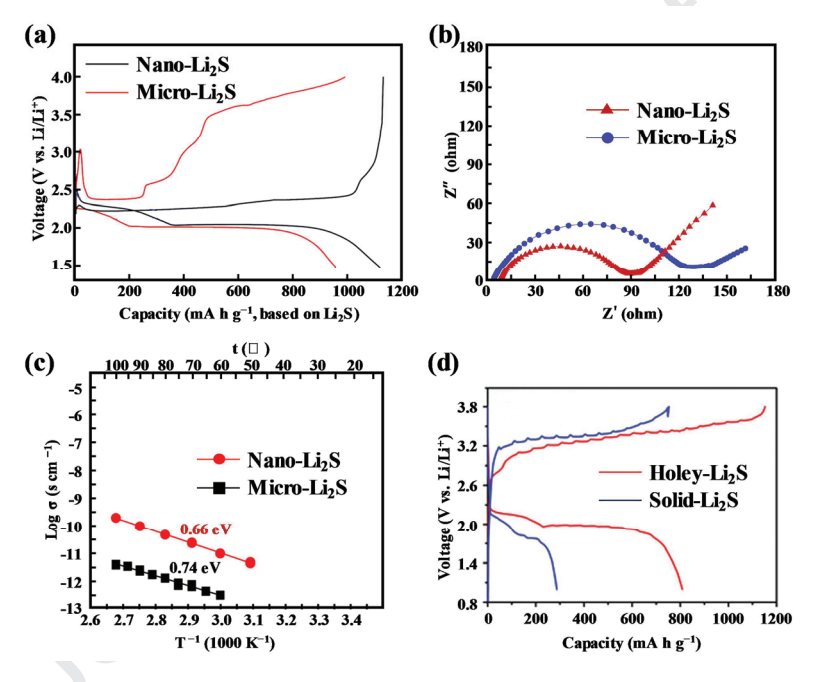


Fig. 5. (a) The initial charging profiles of nano-Li₂S and micro-Li₂S.⁷⁷ Reproduced with permission from Royal Society of Chemistry. (b) Nyquist plots of micro-Li₂S@graphene aerogel and nano-Li₂S@graphene aerogel based fresh electrodes.⁷⁸ Reproduced with permission from Elsevier. (c) Comparison of ionic conductivities corresponding to the micro-Li₂S and nano-Li₂S.⁷⁹ Reproduced with permission from American Chemical Society. (d) The initial charge/discharge profiles of cathodes based on holey-Li₂S and solid-Li₂S at 0.1 C.⁸¹ Reproduced with permission from Wiley.

Morphology is another factor affecting the activation process of Li₂S particles. As shown in Fig. 5 (d), the holey-Li₂S-based cathode presented a 200 mV lower charging voltage than that of solid-Li₂S-based cathode. SEM and XRD characterizations show that Li₂S particles completely disappeared after activation in the holey-Li₂S-based cathodes, while portion of Li₂S particles remained in the solid-Li₂S-based cathode. The holey architecture of Li₂S makes its activation easier to occur due to the increased electrolyte contact area and the enhanced charge transfer between Li₂S and the electrolyte.

In addition to the particle size and the morphology, the crystallinity of Li₂S also plays a critical role in its activation process.⁸² Lithium can be much more easily extracted from amorphous Li₂S than from its crystallites since the bonding force between Li⁺ and S²⁻ is much weaker in an amorphous state than in its crystalline counterpart. Therefore, amorphous Li₂S is more easily oxidized.^{61, 83, 84} For instance, density functional theory-based calculation suggests that 3.21 eV is required to extract a Li atom from Li₂S crystal, in contrast to only 2.18 eV from its amorphous state.⁶¹ As revealed by the electrochemical measurement, a cut-off voltage of 2.8 V is high enough to completely convert amorphous Li₂S to sulfur, while 3.5 V is needed for crystalline Li₂S.⁶¹

2.2.3 Developing host materials

Incorporating Li₂S particles with host materials is another important strategy to lower the initial charge potential barrier. Although the low electronic conductivity of Li₂S plays a negligible role on the initial charging barrier,²² simply encapsulating Li₂S nanoparticles with carbon leads to disappearance of the charge potential barrier.^{85, 86} The critical role of the

carbon shell is to provide a favorable interface for the charge transfer as the reaction happens at the boundary of the three phases of Li₂S, carbon, and the electrolyte.

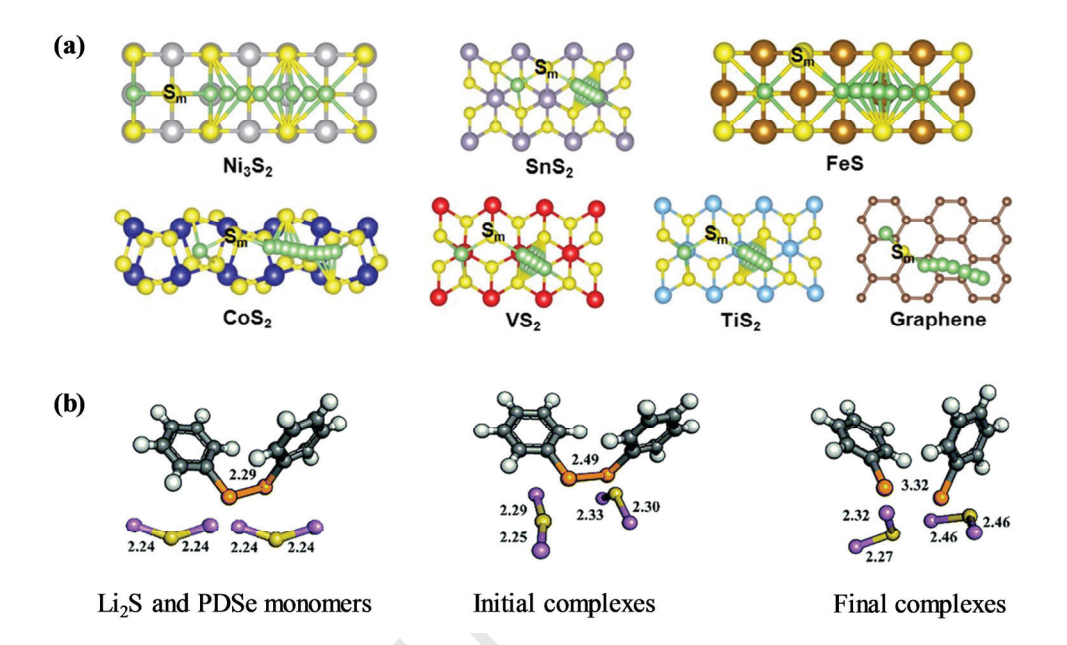


Fig. 6. (a) A schematic illustrating the corresponding decomposition pathways of Li₂S on Ni₃S₂, SnS₂, FeS, CoS₂, VS₂, TiS₂, and graphene, respectively.⁸⁷ Green, yellow, gray, purple, brown, blue, red, cyan, and beige balls symbolize lithium, sulfur, nickel, tin, iron, cobalt, vanadium, titanium, and carbon atoms, respectively. S_m represents the sulfur atom in the Li₂S cluster. Reproduced with permission from National Academy of Sciences. (b) A schematic illustrating the interaction between Li₂S and PDSe.⁸⁸ Green, white, purple, yellow and dark yellow balls symbolize carbon, hydrogen, lithium, sulfur, and selenium atoms, respectively. Reproduced with permission from Royal Society of Chemistry.

The strategy that expedites cleavage or elongation of Li-S bond could also effectively reduce the activation voltage. As revealed by Zhou et al. and Yuan et al., the transition metal

phosphides and sulfides can not only trap the soluble polysulfides, but also effectively catalyze the decomposing of Li₂S to enhance the utilization of active materials.^{87, 89} Compared with a high activation voltage (3.41 V) for a graphene/carbon nanotube-Li₂S structure, the activation potential is 3.01, 2.91, and 2.88 V for CoS₂, VS₂, and TiS₂ based Li₂S cathodes, respectively.⁸⁷ Introduction of Fe₂P, Co₂P, and Ni₂P into Li₂S cathodes also reduce the activation voltage to 2.59, 2.51, and 2.44 V, respectively.⁸⁹ These low dissociation energies of Li₂S are associated with the strong adsorption between Li₂S and metal sulfides or metal phosphides, as shown in Fig. 6 (a).^{87, 89} Similarly, when Li₂S particles are mixed with phenyl diselenide (PDSe), the Se-Se bond of the later will break apart and the attraction between Se and Li will elongate the Li-S bond to 2.46 Å from an original length of 2.24 Å, thereby facilitating the decomposition and oxidation of Li₂S, as shown in Fig. 6 (b).⁸⁸

It deserves to be mentioned that facilitating Li₂S oxidation is extremely important during both the initial activation and the subsequent charging processes. For instance, one major cause of rapid capacity fading in LSBs is the formation of non-soluble Li₂S with relatively low electrochemical activity that blocks electron and Li⁺ transport access.^{90, 91} Therefore, the different methods that can promote Li₂S activation, such as electrolyte additives, Li₂S particle miniaturization and carbon encapsulation would also improve the overall performance of Li₂S cathodes.

3. Producing Li₂S nanoparticles

3.1 Li₂S microparticle based synthesis

Since Li₂S particle size has the dominant impact on its initial activation, great efforts have

been devoted to transforming commercially available Li_2S microparticles to Li_2S nanoparticles, which could be categorized into physical methods and chemical methods.

As one simple physical method, ball milling was used to reduce the particle size.^{22, 51, 92-94} Li₂S particles smaller than 400 nm was achieved by ball milling of as-purchased Li₂S for 6 hours.⁹³ Ball milling is also effective to mix Li₂S particles with carbon matrix for fabricating Li₂S cathodes.^{51, 92, 94} Nevertheless, the obtained Li₂S particles after long-time ball milling is still at the sub-micrometer scale, exhibiting poor electrochemical performance.

Another physical method to attain small Li₂S particles is recrystallization, in which large Li₂S particles are first dissolved in an organic solvent, such as absolute ethyl alcohol, and then recrystallize via solvent evaporation. This convenient method is much more effective than ball milling to achieve fine Li₂S particles. Li₂S particles with a diameter smaller than 100 nm have thus been prepared.^{20, 24, 95-98} In particular, using a modified solution evaporation method, in which Li₂S/ethanol solution was slowly added to polyacrylonitrile/dimethylformamide solution and then Li₂S particles was recrystallized by evaporating the solvent, Hu et al. fabricated ultra-small (~ 5 nm) Li₂S nanoparticles.⁹⁹

Such fine particles of a few nanometers dramatically improve the electrode performance. The cathode combined 3 – 8 nm Li₂S particles with cobalt and nitrogen co-doped carbon delivers an initial specific capacity of 1155.3 mAh g⁻¹ with 929.6 mAh g⁻¹ retained after 300 cycles and demonstrates excellent rate capabilities with 604.1 mAh g⁻¹ released at 4 C.⁹⁶ The superior performance was attributed to the combination of homogeneous distribution of small Li₂S particles and their intimate contact with the carbon matrix.

In addition to these physical methods, chemical methods have also been developed to

produce small Li₂S particles. Li₂S particles with a size ranging from 30 to 500 nm have been produced by the disproportionation of Li₂S₃ or Li₂S₆ solutions. These solutions were prepared by stoichiometric reaction of sulfur and micro-scale Li₂S, and then they were heated above 200 °C to discompose. For this method, the cost and environmental impact resulting from the solvent, including 1, 2-dimethoxyethane (DME) and tetrahydrofuran (THF) might limit its application.

3.2 Li₂SO₄ based synthesis

The carbothermal reduction is considered as an economical approach to produce Li₂S using low-cost lithium sulfate (Li₂SO₄) and carbon or organic materials as precursors. ^{85, 104-106} The obtained Li₂S particle size is largely related to that of Li₂SO₄ precursor. For example, Li₂S particles produced from 2 μm Li₂SO₄ particles that were attained by multi-solvent recrystallization of commercial Li₂SO₄ are much smaller than those prepared directly from commercial Li₂SO₄ that has a particle-size distribution ranging from several micrometers to 30 um. 107 Except for multi-solvent recrystallization, ball milling was also adopted to reduce Li₂SO₄ precursor size for obtaining smaller Li₂S particles. Commercial Li₂SO₄ with a particle size of 300 µm was reduced to 500 nm, 300 nm, and 150 nm via ball milling for 4 hours, 12 hours and 60 hours, respectively. Then $\sim 50 - 150$ nm Li₂S particles were achieved by carbothermally reducing 150 nm Li₂SO₄ particles.⁷² Ball milling was subsequently employed to further reduce the size of as-prepared Li₂S particles. ¹⁰⁸ The temperature for carbothermal reduction is another critical factor in determining the crystallinity and size of Li₂S particles.⁷², 109 The reaction between $\mathrm{Li_2SO_4}$ and carbon could occur above 300 °C according to the Ellingham diagram shown in Fig. 7 (a).⁷² However, the reported carbothermal reduction temperature is around 800 °C in most publications, ^{107, 110} and such a high temperature will promote the particle growth, resulting in large particles with high crystallinity. Recently, Ye et al. found that Li₂S fabricated under a temperature below the melting point of Li₂SO₄, such as 635 °C, could retain the morphology of Li₂SO₄ and even have smaller size (10 – 20 nm) due to the removal of oxygen atoms. ¹⁰⁹ For Li₂S attained under 636 °C, the activation voltage and initial discharging capacity were 2.63 V and 805 mAh g⁻¹, in contrast to 3.2 V and 760 mAh g⁻¹ for that produced at 900 °C. ¹⁰⁹

Organic polymers as the carbon precursors were also used for carbothermal reduction. The highly active and unsaturated carbon bonds, such as those in poly (vinyl alcohol) could promote the low-temperature conversion of Li₂SO₄ to Li₂S particles, ¹⁰⁹ and Li₂S particles with low crystallinity and small size could be achieved under a low temperature. On the other hand, the selected temperature must be high enough so that the used polymer can be simultaneously converted into electronically conductive carbon.

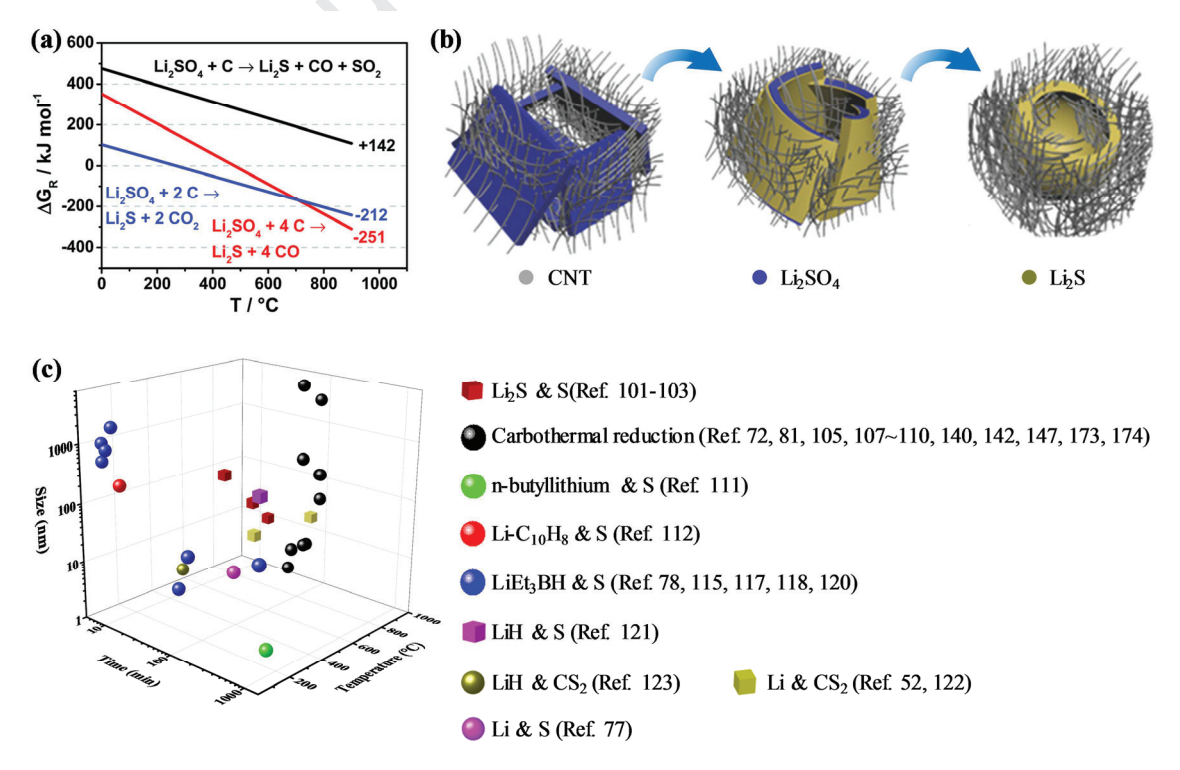


Fig. 7. (a) Ellingham diagram for different carbothermal reductions.⁷² Reproduced with permission from Royal Society of Chemistry. (b) Schematic illustration of the formation process of holey-Li₂S.⁸¹ Reproduced with permission from Wiley. (c) Li₂S particle size, processing time and temperature in various strategies.

Compared to particle size, the effect of Li₂S morphology on its electrochemical performance has not been well investigated. Ye et al. found that holey-Li₂S nanoparticles delivered a much higher specific capacity than solid-Li₂S nanoparticles, whose formation could be explained by the evolution of Li₂SO₄ plates during reaction with near-by carbon nanotube (CNT) matrix, as shown in Fig. 7 (b).⁸¹

3.3 Li and S sources based synthesis

Varieties of methods using economical precursors including sulfur and hydrogen sulfide (H₂S) have also been developed to produce Li₂S. The corresponding lithium sources include n-butyllithium (BuLi), lithium naphthalenide (Li-Naph), lithium hydroxide (LiOH), lithium triethylborohydride (LiEt₃BH) and lithium hydride (LiH).

Yang et al. transformed sulfur particles in CMK-3 carbon with a pore size of sub-5 nm to Li₂S particles with a diameter of 3 – 4 nm by chemically reacting sulfur with BuLi. The size of Li₂S particles is highly related to the pores of carbon host in which sulfur particles are entrapped.

Shen et al. developed a chemical prelithiation strategy using Li-Naph to fully prelithiate sulfur-poly(acrylonitrile) (S-PAN) composite into a Li₂S-PAN cathode which delivered a

specific capacity close to the theoretical capacity.¹¹² The prelithiation process is straight forward by immersing S-PAN in Li-Naph solution and the lithiation degree can be well adjusted by controlling the immersing duration. The sulfur molecules in PAN matrix could be fully transformed to Li₂S after 20 min immersion.¹¹² Li-Naph, as a prelithaition reagent, is relatively stable even when exposed to moist air.

 H_2S can also be converted to Li_2S by reacting with Li-Naph. Li_2S particles with a diameter of 100 nm were prepared via thermodynamically spontaneous reaction between H_2S and Li-Naph, which demonstrated better electrochemical performance than commercial Li_2S in terms of specific capacity, cycling stability, and charge-discharge profile. In this process, only Li_2S is in solid state, and this will facilitate the product purification. Besides, this process provides a strategy to convert "waste" into wealth as the precursor H_2S and the byproduct 1, 4-dihydronaphthalene ($C_{10}H_{10}$) are a major industrial waste and a liquid fuel, respectively. Cost-effective LiOH can also be converted to Li_2S particles by reacting with H_2S via the reaction of 2 LiOH + $H_2S = Li_2S + 2 H_2O$.

Li₂S particles with a diameter ranging from 8.5 nm to 2 μm were prepared via chemically reacting sulfur powder with LiEt₃BH in tetrahydrofuran (THF) according to the chemical equation: S + 2 LiEt₃BH = Li₂S + 2 Et₃B + H₂.^{11,78,79,115-120} As demonstrated by Nan et al., Li₂S particle size could be well adjusted by the reaction time and the amount of toluene used to dissolve sulfur.¹¹⁵ With the same amount of dissolved sulfur, the larger amount of toluene and longer reaction time would lead to larger Li₂S particle size.¹¹⁵ The reaction between sulfur and LiEt₃BH generally results in small Li₂S particles. However, LiEt₃BH is extremely sensitive to air and therefore difficult for practical applications due to safety concern in

addition to its high cost.

Li et al. reported a novel mechanochemical method to synthesize Li_2S with submicron size by ball-milling lithium hydride (LiH) with sulfur for 24 h in Ar atmosphere at room temperature. The reaction, 2 LiH + S = Li_2S + H_2 , has a Gibbs free energy of -211 kJ mol⁻¹ at room temperature. It may be difficult to achieve pure Li_2S via this reaction as LiH, sulfur, and Li_2S are all solids.

Other strategies such as the reaction of CS₂ and LiH or Li,^{52, 122, 123} the reaction of lithium and sulfur,⁷⁷ and the electrochemical method,¹²⁴ can produce Li₂S nanoparticles directly encapsulated in carbon shell or a polymeric gel-like film. They will be discussed in Section 5 "Simultaneously Producing and Encapsulating Li₂S Nanoparticles".

In a nutshell, great efforts have been devoted to synthesizing Li₂S nanoparticles that are desirable for enhancing the electrochemical performance. Nevertheless, small Li₂S particles tend to aggregate, and great attention must be paid to prevent it from happening. Otherwise, much larger clusters will be formed, resulting in much worse performance. The slower activation kinetics for nominal 500 nm Li₂S particles than 1 μm particles suggests longer Li diffusion distances for the former particles than the latter one, which could be attributed to significant agglomeration of 500 nm Li₂S particles after high-temperature treatment. Therefore, producing small Li₂S particles and improving their dispersion both are critical. Although nanoscale Li₂S particles might offer better electrochemical kinetics due to their increased interfacial area with electrolyte and conductive additives, their practical application, particularly their storage after synthesis faces much more challenge than that of microscale particles because nanoparticles with a large surface area could be contaminated more easily,

resulting in undesirable thermal runaway and toxic hydrogen sulfide generation.⁵⁶ The Li₂S particle sizes, synthetic time and temperature using different methods are summarized in Fig. 7 (c). The precursors and corresponding chemical reactions are listed in Table 1.

Compared to Li₂S particle size tailoring, studies on particle morphology and crystallinity engineering are very scarce even though these two properties of Li₂S particle most likely play similar roles as the particle size in determining the electrochemical kinetics. The very few studies include fabrication of holey-Li₂S via delicately designed carbothermal reduction, and preparation of amorphous Li₂S via in-situ Li₂S₈ discharging. There might exist enough room to further prompt the electrochemical performance of Li₂S cathodes through morphology and crystallinity engineering of Li₂S.

Table 1 Precursors and chemical reactions for different Li₂S preparation methods.

Precursors	Reaction
Li ₂ S & Sulfur	$\text{Li}_2\text{S}_3 \rightarrow \text{Li}_2\text{S} + 2 \text{ S}$
Li ₂ S & Sulfur	$\text{Li}_2\text{S}_6 \rightarrow \text{Li}_2\text{S} + 5 \text{ S}$
Li ₂ SO ₄ & carbon	$\text{Li}_2\text{SO}_4 + 2 \text{ C} \rightarrow \text{Li}_2\text{S} + 2 \text{ CO}_2$
N-butyllithium & Sulfur	$2 C_4H_9Li + S \rightarrow Li_2S + C_4H_9-S-C_4H_9$
Lithium & C ₁₀ H ₈ & Sulfur	$2 \text{ Li-C}_{10}\text{H}_8 + \text{S} \rightarrow \text{Li}_2\text{S} + 2 \text{ C}_{10}\text{H}_8$
Lithium & C ₁₀ H ₈ & H ₂ S	$2 \text{ Li-C}_{10} H_8 \ + \ H_2 S \ \rightarrow \ \text{Li}_2 S \ + \ \text{C}_{10} H_{10} \ +$
	$C_{10}H_{8}$
LiOH & H ₂ S	$2 \text{ LiOH} + \text{H}_2\text{S} \rightarrow \text{Li}_2\text{S} + 2 \text{ H}_2\text{O}$
LiEt ₃ BH & Sulfur	$2 \text{ LiEt}_3\text{BH} + \text{S} \rightarrow \text{Li}_2\text{S} + 2 \text{ Et}_3\text{B} + \text{H}_2$

LiH & Sulfur	$2 \text{ LiH} + S \rightarrow \text{Li}_2S + \text{H}_2$
LiH & CS ₂	$4 \text{ LiH} + \text{CS}_2 \rightarrow 2 \text{ Li}_2\text{S} + \text{C} + 2 \text{ H}_2$
Lithium & CS ₂	$4 \text{ Li} + \text{CS}_2 \rightarrow 2 \text{ Li}_2\text{S} + \text{C}$
Lithium & Sulfur	$2 \text{ Li} + \text{S} \rightarrow \text{Li}_2\text{S}$
MoS_2	$MoS_2 + x Li^+ + x e^- \rightarrow Li_x MoS_2 (0.6 V \le$
	$U < 1.2 \text{ V vs. Li/Li}^+$
	$Li_xMoS_2 + (4-x) Li^+ + (4-x)e^- \rightarrow Mo + 2$
	Li_2S (0.01 V \leq U $<$ 0.6 V vs. Li/Li^+)

4. Encapsulating Li₂S nanoparticles

Due to its poor electronic and ionic conductivities, a matrix with high electronic and ionic conductivities to encapsulate Li₂S nanoparticles is necessary to establish paths for electron and Li⁺ transport as well as enhancing the charge transfer rate at the active materials/electrolyte interface. Simultaneously, this matrix could also serve as a physical and/or a chemical barrier to hinder soluble Li₂S_x from diffusing out of the cathode and thus elevating the utilization of active materials and reducing the adverse shuttle effects. All the encapsulation or trapping principles for the sulfur cathode are the same no matter elemental sulfur or Li₂S is used as the starting material. However, the encapsulation process for these two materials is different due to their different properties. Unlike elemental sulfur, the rigidity of Li₂S makes it difficult to encapsulate Li₂S particles with common carbon hosts via ball milling. With its high melting point and low vapor pressure, it is also difficult for Li₂S to diffuse into nanopores of the matrix through capillary effect. Nevertheless, the high melting

point of Li₂S provides opportunities for other encapsulation methods that cannot be used for elemental sulfur encapsulation. These methods could be classified into three categories according to the encapsulation process: mixing and pyrolysis-based carbon encapsulation, chemical vapor deposition-based carbon encapsulation, and surface chemical reaction-based encapsulation.

4.1 Mixing and pyrolysis-based carbon encapsulation

Various polymers or ionic liquids can be applied to uniformly mix with Li₂S on account of their viscosity, and the subsequent pyrolysis at a high temperature under inert atmosphere will result in a carbon coating on Li₂S particles. Suo et al. applied a flowable ionic liquid as a carbon precursor to encapsulate Li₂S nanoparticles with a uniform and dense carbon film. 117 The obtained ideal encapsulation was attributed to the high mobility of the selected ionic liquid resulting in sufficient immersion of Li₂S particles. The carbon-coated Li₂S demonstrated long cycling stability with Coulombic efficiency approaching 100%. Liu et al. also coated Li₂S particles with a carbon layer using a similar method to enhance its electronic conductivity and alleviate the diffusion of Li₂S_x. ¹⁰⁷ Carbon coating on Li₂S particles can also be implemented by pyrolysis of polymers including polyacrylonitrile (PAN), polystyrene (PS) and polyvinylpyrrolidone (PVP). 86, 119, 121, 125, 126 The Li₂S particles embedded in carbon coating derived from PAN or PS have a diameter of a few to tens of nanometers although they had an initial size of sub-micrometers, 121, 125 implying that this encapsulation process via pyrolysis simultaneously decreases the size of Li₂S particles. Li₂S encapsulated with PVP-derived carbon has an electronic conductivity of 5.6×10^{-5} S cm⁻¹, much higher than that of bare Li₂S ($\sim 10^{-13}$ S cm⁻¹). ¹²⁶ As a high temperature (> 600 \square) is required to convert

Journal Pre-proof

polymers to carbon with high electronic conductivity, this encapsulation strategy can be applied to Li₂S with a high melting point, while not appropriate for sulfur.

4.2 Chemical vapor deposition-based carbon encapsulation

Chemical vapor deposition (CVD) is another approach to encapsulate Li₂S particles. A thin carbon layer could be coated on Li₂S particles by decomposing acetylene (C₂H₂) to protect Li₂S from direct contact with electrolyte, thereby inhibiting the shuttling effects of lithium polysulfides, ^{115, 116, 118} as shown in Fig. 8 (a) - (c). The thickness could be well controlled by the time of exposure to the argon-acetylene atmosphere. ¹¹⁵ Compared with conventional CVD, rotating the CVD furnace (Fig. 8 (d)) can enhance the uniform encapsulation of Li₂S particles and lead to strong confinement of Li₂S_x (Fig. 8 (e)). ^{118, 127} The high decomposing temperature of C₂H₂ makes this strategy feasible for Li₂S, but not for sulfur.

4.3 Surface chemical reaction-based encapsulation

The reaction between surface of Li₂S with other chemicals would provide a simple strategy to encapsulate Li₂S nanoparticles. Metal sulfides, Li₃PS₄, and LiTiO₂ have been coated on Li₂S nanoparticles through surface chemical reaction.

As carbon cannot well bind with Li₂S through chemical bonds due to their different polarities, other encapsulation materials are needed. Seh et al. developed a conductive and polar coating to encapsulate Li₂S particles through chemical reaction of TiCl₄ on Li₂S particle surface: TiCl₄ + 2 Li₂S \rightarrow TiS₂ + 4 LiCl, as shown in Fig. 8 (f). The TiS₂ coating elevated

the electronic conductivity to 5.1×10^{-3} S cm⁻¹, around 10 orders of magnitude higher than that of bare Li₂S (10⁻¹³ S cm⁻¹). Besides as a physical barrier, this TiS₂ shell also chemically interacts with sulfur species through the S atoms in TiS2 and Li atoms in Li2Sx. This strategy can be expanded to other transition metal disulfides including ZrS2 and VS2 by reacting Li2S with ZrCl₄ or VCl₄, respectively. ¹²⁸ In addition to effectively confining Li₂S_r in the host material, the shuttle effect could also be alleviated by accelerating Li_2S_x redox kinetics which is even more effective than the former. 129, 130 Transition-metal sulfides have been proven to be a highly efficient electrocatalyst and absorbent for polysulfides.^{87, 128, 131, 132} Many electrocatalyst-related studies have been conducted using sulfur-based cathodes, but similar studies in Li₂S-based cathode are sparse. 133-136 Considering the high-temperature processing ability of Li₂S, rationally designed Li₂S cathode structure with electrocatalysts shall be much easier to implement, and as such, there might be more opportunities here. The disadvantage of introducing electrocatalysts including metal sulfides and oxides into cathodes is that their large mass density and low specific surface area might limit the achievable specific capacity.

In addition to electronic conductivity, the enhancement of Li^+ conductivity in $\mathrm{Li}_2\mathrm{S}$ cathodes is also highly desired. Lithium phosphorus sulfide ($\mathrm{Li}_3\mathrm{PS}_4$) is considered as an excellent solid-state electrolyte due to its high ionic conductivity, low electrochemical activity, and effectiveness in preventing the formation of lithium dendrite. Therefore, using $\mathrm{Li}_3\mathrm{PS}_4$ coating to encapsulate nano-scale $\mathrm{Li}_2\mathrm{S}$ was studied by surface reaction of $\mathrm{Li}_2\mathrm{S}$ particles with $\mathrm{P}_2\mathrm{S}_5$ according to 3 $\mathrm{Li}_2\mathrm{S} + \mathrm{P}_2\mathrm{S}_5 = 2 \mathrm{Li}_3\mathrm{PS}_4$ (Fig. 8 (g)). The $\mathrm{Li}_3\mathrm{PS}_4$ shell can enhance the ionic conductivity of $\mathrm{Li}_2\mathrm{S}$ nanoparticles from $\mathrm{10}^{-11}$ to $\mathrm{10}^{-7}$ S cm⁻¹ at 25 °C. As compared with $\mathrm{Li}_2\mathrm{S}$ particles, the $\mathrm{Li}_2\mathrm{S}@\mathrm{Li}_3\mathrm{PS}_4$ core-shell structure demonstrated

excellent electrochemical performance in all-solid LSBs (Fig. 8 (h)). Functioning as an ionically conductive coating on Li_2S particles and the solid electrolyte of the cell, Li_3PS_4 would simultaneously avoid the shuttling of lithium polysulfides and the safety issues resulting from the lithium dendrite growth.

Both electronic and lithium ionic conductivities play critical roles in the electrochemical performance of Li₂S cathodes. LiTiO₂, as a mixed ionic-electronic conductor, can simultaneously enhance the electronic and lithium ionic conductivity of Li₂S cathodes. Furthermore, the polar Ti–O units in LiTiO₂ have a high affinity for Li₂S_x, thereby alleviating their diffusion. A uniform LiTiO₂ layer with a thickness of 10 nm was coated on Li₂S nanoparticles via the reaction between surface Li₂S and TiO₂ at 650 \Box : 2 TiO₂ + Li₂S = 2 LiTiO₂ + S↑. Due to its unique structure, Li₂S@LiTiO₂ cathode with 4.8 mg cm⁻² Li₂S presented impressive performance with an initial capacity of 585 mAh g⁻¹ at 0.5 C and a capacity retention of 92 % after 200 cycles. Description of 92 % after 200 cycles.

Admittedly, the encapsulation of Li₂S particles with electronically or lithium ionically conductive matrix can enhance the electrochemical performance of LSBs. However, it must be emphasized that the composite nanostructure should be properly designed so that the active Li₂S occupies a high content and a high loading in the composite electrode. Otherwise, the achievable specific energy of LSBs might not surpass that of LIBs.⁸

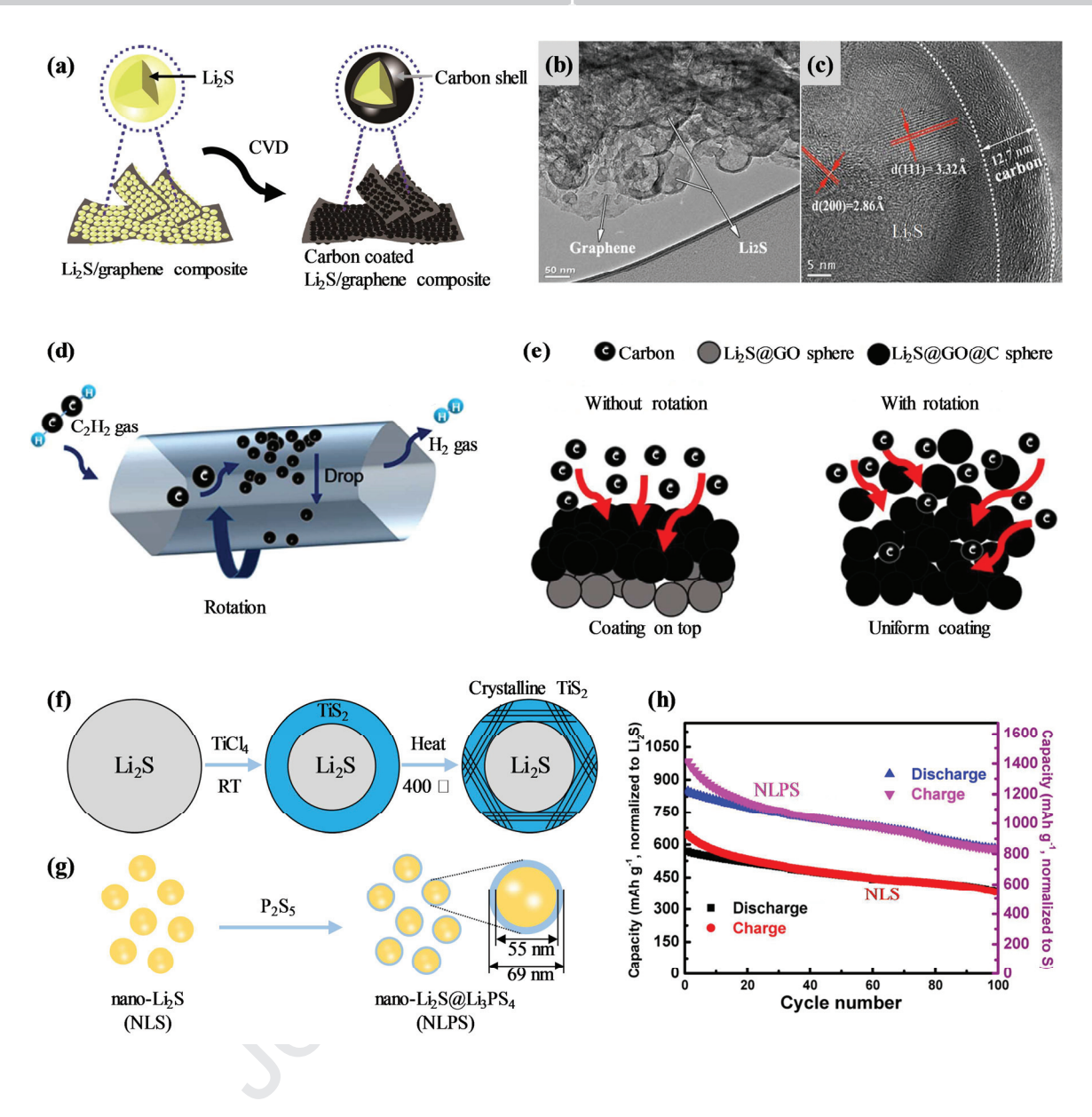


Fig. 8. (a) Schematic illustration of Li₂S particles encapsulated by a carbon shell.¹¹⁶ (b) Low magnification and (c) high-resolution TEM image of the carbon-coated Li₂S/graphene composite.¹¹⁶ Reproduced with permission from Elsevier. (d) Schematic illustrating the carbon coating process using a rotating CVD furnace.¹¹⁸ (e) Schematic illustrating the difference in carbon coating effects under the conventional CVD method and modified CVD method using the rotating furnace.¹¹⁸ Reproduced with permission from American Chemical Society. (f) Schematic illustration of Li₂S particles with a TiS₂ shell.¹²⁸ Reproduced with

permission from Nature Publishing Group. (g) Schematic illustration of Li₂S particles with a Li₃PS₄ shell.⁷⁸ Reproduced with permission from Elsevier. (h) Cycling performance of nano-Li₂S and nano-Li₂S@Li₃PS₄.⁷⁹ Reproduced with permission from American Chemical Society.

5. Simultaneously producing and encapsulating Li₂S nanoparticles

Compared to the two-step process in which nanoparticles are first produced and then encapsulated, a one-step process in which Li₂S nanoparticles are produced and simultaneously encapsulated into a host is more desirable. This can obtain much better encapsulation, and also minimize the possibility of Li₂S exposure to air. Additionally, a one-step process shall reduce fabrication cost and improve productivity.

5.1 Polymer pyrolysis based synthesis

Due to their viscous property, polymers are an excellent material for uniformly mixing reactants and serving as the precursor for carbon encapsulation. Ye et al. prepared nanofibers containing Li_2S_3 and PVP by electrospinning and subsequently attained Li_2S @carbon nanofibers by decomposing Li_2S_3 and pyrolyzing PVP.¹⁰¹ The Li_2S particles with a grain size of 60-80 nm were encapsulated by the PVP-derived carbon.

As a matter of fact, carbothermal reduction with polymer as the carbon precursor is a common method that produces encapsulated Li₂S particles in one-step process and therefore simplifying the process of Li₂S composite production. In one study, composites of Li₂SO₄, resorcinol formaldehyde (RF) and CNTs were prepared using spray drying method and then pyrolyzed to attain Li₂S@carbon@CNT.¹⁴⁰ CNTs were used to facilitate the uniform

distribution of Li₂SO₄ and thereby contribute to achieve highly dispersed and small Li₂S particles, and also serve as an excellent electron transport network. Yang et al. reported the in-situ synthesis of Li₂S@carbon by pyrolyzing composite of Li₂SO₄ and RF.¹⁴¹ The homogeneous distribution of Li₂S in the carbon matrix could be attributed to the specific interaction of Li₂SO₄ precursor for Li₂S and polar oxygens in RF for carbon. Since the chemical bonding between the heteroatom-doped carbon and Li₂S_x can alleviate the shuttling effect, organic materials containing N or P present great advantages as the carbon precursors.¹⁴²⁻¹⁴⁶ Besides, Zhang et al. demonstrated N, P-doped carbon could enhance the ionic conductivity of Li₂S by forming Li_xPS_y.¹⁴² Recently, Li₂S particles smaller than 5 nm were entrapped in N-doped carbon cages embedded with ZnS particles via confining Li₂SO₄ into metal-organic molecular cages first and then pyrolyzing the composite (Fig. 9 (a)), ¹⁴⁷ The ZnS particles demonstrate distinct electrocatalytic effect on Li₂S dissociation as well as strong chemisorption for sulfur species.¹⁴⁷

5.2 CS₂ based synthesis

Chemical reactions that produce Li₂S and carbon provide an ideal strategy for producing composites of Li₂S and carbon. Reactions between lithium and CS₂, and between LiH and CS₂ are two examples, which theoretically can produce Li₂S and carbon composites with Li₂S ratios of 79.3 wt% and 88.5 wt%, respectively, according to their chemical equations provided that all Li and LiH are fully reacted. As demonstrated by Yan et al. and Tan et al., 50 – 100 nm Li₂S particles wrapped by few-layer graphene (Li₂S@C) were prepared via combusting lithium foil in CS₂. 52, 122 The Li₂S@C composite demonstrated 91% of Li₂S utilization when applied as the cathode in all-solid-state LSBs despite of an ultrahigh Li₂S

loading of 7 mg cm⁻².¹²² The Li₂S@C composite can enhance the charge transfer at the cathode/electrolyte interface, and the graphene layer can accommodate the large volume change of Li₂S during cycling and inhibit the aggregation of Li₂S. When applied in liquid-electrolyte LSBs, Li₂S@C delivers a high reversible specific capacity of 807 mAh g⁻¹ in spite of a high Li₂S loading of 10 mg cm⁻², corresponding to an areal capacity of 8.1 mAh cm⁻².⁵² The Li₂S content in Li₂S@C prepared via reaction between LiH and CS₂ is as high as 88.7 wt%, ¹²³ agreeing well with the calculation based on the chemical equation. Due to its unique architecture with Li₂S core entrapped in a porous carbon shell, Li₂S@C demonstrated excellent cycling stability and superior rate performance. ¹²³

5.3 Confined lithium or sulfur nanoparticle based synthesis

Li₂S can also be prepared by chemical reaction of lithium with sulfur. As reported by Chen et al., the direct reaction between lithium foil and sulfur results in 280 nm Li₂S particles, while core-shell Li₂S@C particles with the Li₂S core of 20 – 40 nm and the carbon shell of 0.8 nm thick are achieved by initially transforming lithium foil to core-shell Li@C particles via plasma sparking and then sulfurizing Li@C, as shown in Fig. 9 (b) and (c).⁷⁷ For the Li₂S@C core-shell particles, the nano-scale Li₂S core can shorten the lithium-ion diffusion path and facilitate the electrochemical charge transfer kinetics, while the carbon shell can enhance the electronic conductivity of the Li₂S cathode and impede the diffusion of Li₂S_x. Similarly, encapsulated Li₂S particles were also fabricated by in situ lithiated sulfur particles entrapped in microporous carbon using commercial stabilized lithium metal powder.¹⁴⁸

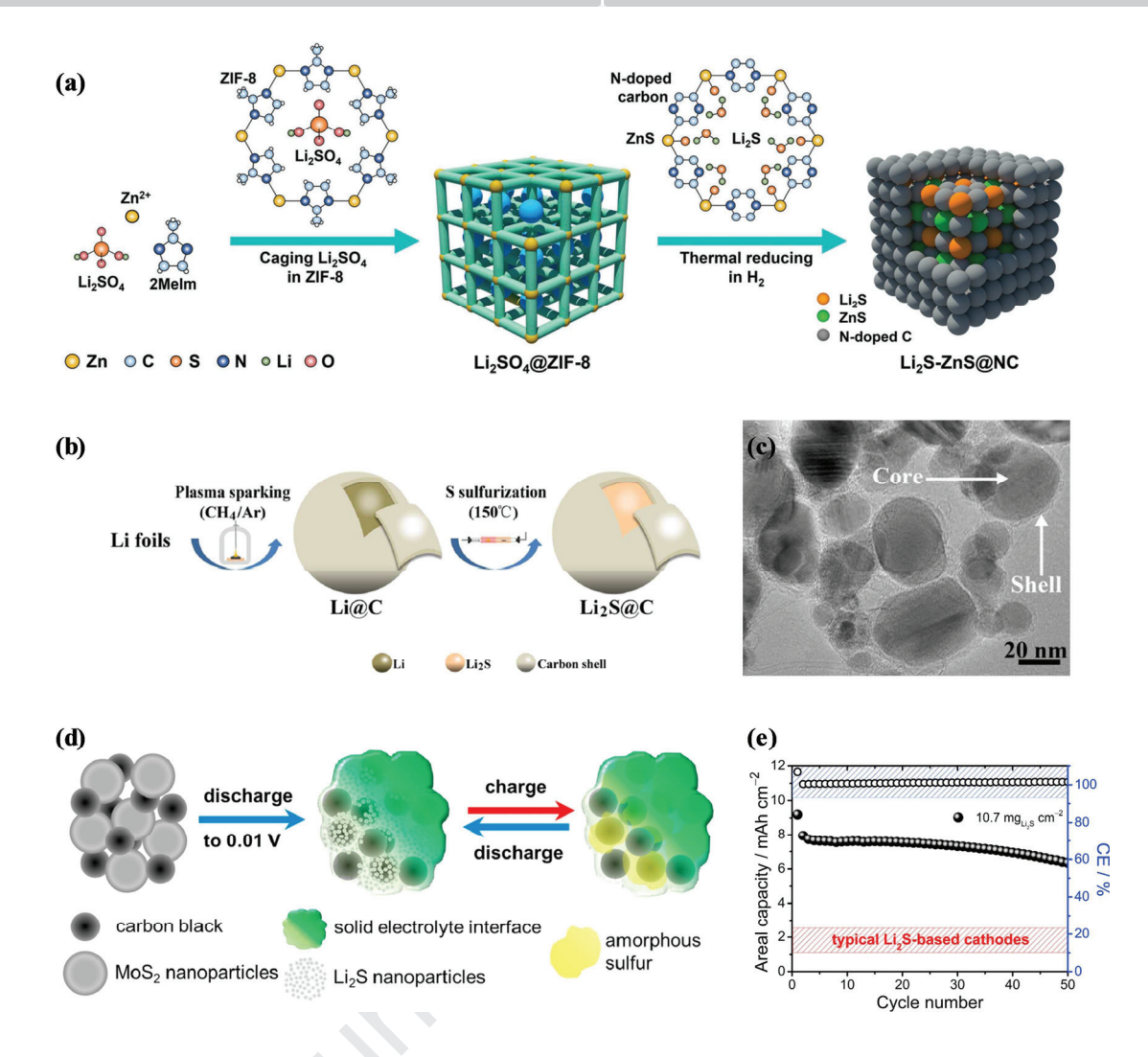


Fig. 9. (a) Schematic illustrating the synthesis process of Li₂S-ZnS@NC.¹⁴⁷ Reproduced with permission from Wiley. (b) Schematic illustrating the synthesis of Li₂S@C and (c) TEM image of Li₂S@C.⁷⁷ Reproduced with permission from Royal Society of Chemistry. (d) Schematic illustrating the simultaneous synthesis and encapsulation of Li₂S using electrochemical method and (e) cycling performance of the Li₂S cathode attained using electrochemical method.¹²⁴ Reproduced with permission from Elsevier.

5.4 Electrochemical method based synthesis

Different from chemical reactions, an electrochemical method to produce and encapsulate Li₂S particles has also been reported. By deeply discharging MoS₂ nanoparticles in a carbonate-based electrolyte, Balach et al. produced ultra-small Li₂S nanoparticles (15 nm) embedded in a highly-stable polymeric gel-like SEI film derived from the electrolyte decomposition during the discharge process (Fig. 9 (d)). 124 The gel-like film, serving as a SEI layer in lithium-ion and sodium-ion batteries, is typically formed by decomposition of the carbonate-based electrolyte during the discharge process. 149, 150 The generated metal particles (Mo) in the Li₂S matrix can enhance the electronic conductivity of Li₂S cathodes. ¹⁵¹ As shown in Fig. 9 (e), the battery with 10.7 mg cm⁻² of Li₂S delivered an outstanding areal capacity of 7.5 mAh cm⁻². ¹²⁴ Similar to Li₂SO₄, the size of MoS₂ also plays a critical role on the electrochemical performance of MoS₂-derived Li₂S cathodes. The Li₂S cathode prepared from MoS₂ nanoparticles performed much better than that from MoS₂ micro-sized particles. 124 When the MoS₂ particles were initially encapsulated by reduced graphene oxide (RGO), the achieved Li₂S particles via lithiating MoS₂ to 0.01 V vs. Li/Li⁺ were also entrapped by RGO. 152 In spite of a high Li₂S loading (5 mg cm⁻²), the obtained cathode exhibits a high initial capacity of 975 mAh g⁻¹ (based on Li₂S mass) at 0.1 C and a small capacity decay rate of 0.18% per cycle during 200 cycles at 2 C. 152

As we know, sulfur cathodes are incompatible with carbonate-based electrolytes since the nucleophilic Li_2S_x intermediates tend to react with the electrophilic carbonate-based solvents through a nucleophilic addition or substitution reaction, resulting in rapid capacity decay of LSBs. ^{153, 154} Only a few publications reported the successful operation of sulfur cathodes based on chain sulfur (S₂₋₄) or cyclo-S₈ in carbonate-based electrolytes. ¹⁵⁵⁻¹⁵⁸ All these sulfur

cathodes, with sulfur covalently bonded and/or physically confined in the host materials, demonstrated a direct conversion between sulfur and Li_2S . However, the reason why the generation of Li_2S_x is circumvented is still under debate and need further investigation. ^{156, 159}

As the electrochemical process of Li₂S-based cathode is similar to sulfur cathode, with lithium polysulfides as intermediates, Li₂S-based cathode also does not match carbonate-based solvents. However, Juan et al. reported a facile strategy of preparing Li₂S particles compatible with carbonate-based electrolytes, as they are entrapped in polymeric gel-like film and generation of Li₂S_x does not exist. 124, 152

Noteworthily, substituting the conventional ether-based electrolytes with carbonate-based would expand the operation voltage of LSBs. The drawback of using ether-based electrolytes with a volatile nature could be circumvented by selecting carbonate-based electrolytes with a higher boiling point. In addition, the notorious shuttle effect resulting from dissolved Li₂S_x could be effectively averted with the delicately designed sulfur- or Li₂S-based cathodes operating in carbonate-based electrolytes.

6. Fabricating Li₂S cathodes

Similar to sulfur cathodes, Li₂S cathodes have been fabricated by either casting their slurry on a current collector or they are created as a free-standing structure. An interlayer, whose function was discovered by Manthiram et al. when studying the sulfur cathode, ¹⁶¹⁻¹⁶³ has also been incorporated on the Li₂S cathode to improve its overall electrochemical performance.

6.1 Slurry-casting-based cathodes

Slurry casting of active materials on a metallic foil-based current collector is a conventional process to fabricate electrodes used in many electrochemical cells. ¹⁶⁴⁻¹⁶⁸ Specifically, active material, conducting agent, and binder are mixed in a solvent to form slurry, which is then casted on the current collector to form the electrode. As for sulfur-based cathodes, this process could be performed in the atmosphere due to the chemical inertness of sulfur in it. Nevertheless, as for Li₂S cathodes, the time-consuming slurry preparation and casting process will result in serious contamination of Li₂S due to its reaction with moisture. Thus, Li₂S cathodes should be fabricated in an argon glovebox in the laboratory. ^{140, 169} In the current lithium-ion battery manufacturing plant, the relative humidity is generally controlled to be 30% for electrode fabrication process. Even for the more reactive Ni-rich positive electrodes, it is merely controlled to be 10%. Thus, it should be evaluated whether the current production environment is appropriate for Li₂S slurry preparation and its casting process for LSB manufacturing.

Dressel et al. developed an approach to avoid the contamination. Specifically, the slurry containing LiOH, carbon black, and binder was coated on a current collector, which was then heated at $100 \square$ or $150 \square$ for 1 h under H₂S atmosphere to convert LiOH into Li₂S. Thereby, the exposure of Li₂S to air was effectively averted. However, this method does not have the flexibility in controlling Li₂S nanoparticles.

6.2 Free-standing cathodes

Fabrication of free-standing electrodes is regarded as a better method to use well-controlled Li₂S nanoparticles and avoid their contamination. The adoption of free-standing electrodes also makes metal foil current collector unnecessary, thereby reducing

the fabrication cost and enhancing the practical energy density. The strategies to construct free-standing Li₂S cathodes can be generally classified into two categories. In the first category, as shown in Fig. 10 (a), 170 self-supporting host materials are fabricated into a carbon-based porous network, which is then infiltrated with a solution containing Li₂S particles, followed by recrystallization of Li₂S in the carbon host. The host materials could be carbon felt. 97 carbon cloth decorated with vertical-aligned graphene. 24 RGO paper. 26 graphene aerogel, 78, 171 etc. In the second strategy, precursors for the Li₂S/C composite are molded into a free-standing slice and then is thermally treated to attain the free-standing Li₂S/C electrode. The precursors are mainly composites of Li₂SO₄ with carbon materials or polymers. 106, 109, 172, 173 For example, Yu et al. reported the fabrication of flexible sheets composed of Li₂SO₄@PVP nanofibers using an electrospinning method, which were converted into flexible electrodes composed of Li₂S@nitrogen-doped carbon nanofiber via a carbothermal reduction reaction (Fig. 10 (b)). 174 With these preformed sheets, electrodes with different thicknesses for different areal capacities can be easily achieved by stacking several sheets together with no concerns on the detach of active materials from the current collector, a common issue for electrodes made from the slurry-casting method. Along with increase of layers, specific capacity of the electrode only exhibited small reduction (Fig. 10 (c)). 174 It deserves to be mentioned that the mechanical property of the free-standing electrodes should be strong enough for stretching and rolling during the assembling process.

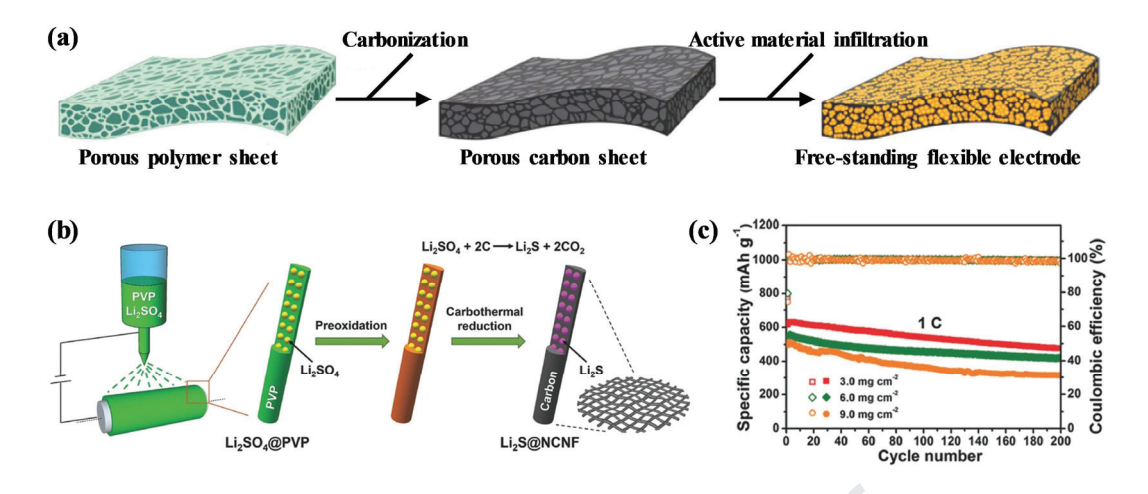


Fig. 10. (a) Schematic illustrating the fabrication of freestanding Li₂S cathode via infiltration.¹⁷⁰ Reproduced with permission from Wiley. (b) Schematic illustrating the fabrication process of freestanding Li₂S cathode via electrospinning and subsequent pyrolysis.¹⁷⁴ Reproduced with permission from Wiley. (c) Cycling performance and Coulombic efficiency of Li₂S@NCNF electrodes with Li₂S loading of 3.0, 6.0, and 9.0 mg cm⁻² at 1.0 C.¹⁷⁴ Higher loading was realized by simply stacking more layers of Li₂S@NCNF paper. Reproduced with permission from Wiley.

6.3 Interlayer and coating layer

For LSBs, no matter the starting material of the cathode is sulfur or Li₂S, the charge-discharge cycling always proceeds along the conversion between sulfur and Li₂S. To retard the diffusion of lithium polysulfides out of the electrode, the concept of interlayer, developed for sulfur-based cathodes, ¹⁷⁵⁻¹⁷⁷ is also suitable for Li₂S cathodes. For example, a nitrogen-doped CNT film was applied on top of the free-standing Li₂S cathode to hinder the diffusion of Li₂S_x. ¹⁷⁸ Similarly, a graphene film covering the Li₂S cathode was used to

restrain Li₂S_x. ¹⁷⁹ Different from sulfur-based cathodes, this blocking layer can be directly formed on the Li₂S cathodes due to the high melting temperature of Li₂S. A thin carbon layer, derived from decomposition of acetylene in a CVD process, was coated on the surface of freestanding Li₂S cathode (P-Li₂S) to achieve P-Li₂S@C. ¹⁷³ The P-Li₂S@C cathode demonstrates much better electrochemical performance than P-Li₂S in terms of cycling stability and rate capability. ¹⁷³ The Nyquist plots show that P-Li₂S@C cathode possesses smaller charge transfer resistance and Warburg impedance than P-Li₂S, indicating that the carbon coating by CVD facilitates charge- and ion-transfer. ¹⁷³ In another study, Chen et al. grew a thin Al₂O₃ film on freestanding Li₂S@graphene slice. ¹⁷² The Al₂O₃ film physically confined Li₂S_x and chemically bound them to enhance the utilization of active materials. The application of a coating on the self-supporting Li₂S cathode or an interlayer between the Li₂S cathode and separator has proved to be effective in improving the electrochemical performance.

Although lithium metal anodes are still far from practical application due to several problematic issues especially the lithium dendrite growth, ^{180, 181} the electrochemical performance of cells using a Li₂S cathode against a lithium metal anode does reflect the quality of a Li₂S cathode structure. Some representative works on Li₂S cathodes in the literature are summarized in Table 2.

Table 2. Electrochemical performance of Li₂S cathodes.

Producing Li ₂ S	Host material	Freestanding (Y or N)	Li ₂ S content (wt%)	Li ₂ S loading (mg cm ⁻²)	Initial capacity (mAh g ⁻¹)	Cycle number	Decay rate (%)	Current density (C)	Ref.
Milling micro-Li ₂ S	Carbon black	N	70	2.3	590	60	0.59	0.05	50
Milling micro-Li ₂ S	Carbon black	N	38	1 – 1.5	858	100	0.22	0.1	22
Milling micro-Li ₂ S	Pyrrole-deriv ed carbon	N	72	1	1029	100	0.366	0.2	93
Milling micro-Li ₂ S	Polystyrene-d erived carbon	N	46.5	0.47	971	200	0.18	0.1	125
Milling micro-Li ₂ S	CNT	N (W/ CNT interlayer)	49	3.5	888	100	0.493	0.1	92
Milling micro-Li ₂ S	TiS ₂	N	51	1	666	400	0.058	0.5	128
Recrystallizing Li ₂ S	Carbon layer through CVD	N	57.8	2.8	754	200	0.15	0.2	95
Recrystallizing Li ₂ S	PVP-derived carbon	N	51	1.4	922	100	0.095	0.2	182
Recrystallizing Li ₂ S	PAN-derived carbon	N	40	1.77	355	50	0.43	0.02	15
Recrystallizing Li ₂ S	PAN-derived carbon	N	63	_	958	1000	0.041	0.5	99
Recrystallizing Li ₂ S	Graphene & carbon layer through CVD	N	55	1.3	723	700	0.004	0.5	183
Recrystallizing Li ₂ S	Pyrrole- derived carbon	N	60	0.8 – 1	637	200	0.18	0.2	20

		D			αf
ourn	aı			U	OI.

Recrystallizing Li ₂ S	ZIF-67-derive	N	41.6	2	1137	300	0.06	0.2	96
Recrystallizing Li ₂ S	LiTiO ₂	N	57.6	1.2	730	400	0.03	0.5	139
Recrystallizing Li ₂ S	Graphene	Y	50	1	853	300	0.041	0.2	184
Recrystallizing Li ₂ S	MXene/ graphene aerogels	Y	62	3	710	200	0.133	0.2	27
Recrystallizing Li ₂ S	MWCNT	Y	30	0.9	843	100	0.16	0.2	98
Recrystallizing Li ₂ S	RGO & PVP-derived Carbon	Y	75	2.5 – 3.5	456	200	0.08	1	86
Recrystallizing Li ₂ S	RGO	Y	50 – 60	0.8 – 1.5	1119	150	0.18	0.1	26
Recrystallizing Li ₂ S	Vertical graphene	Y (W/ carbon coating)		1.84	890	100	0.26	0.1	24
Recrystallizing Li ₂ S	Carbon felt	Y (W/ carbon coating)	-	7	747	200	0.12	1	97
Recrystallizing Li ₂ S	Cellulose-deri ved carbon	Y (W/ carbon coating)	50	1.3	878	400	0.058	0.5	170
Decomposing Li ₂ S ₃	Nitridated graphene	N	60	1.2	817	500	0.082	0.2	103
Decompose Li ₂ S ₆	RGO	N	52.8	0.96	982	100	0.68	0.1	102
Carbothermal reduction	PVP & P-PANI-deriv ed carbon	N	62	2	1000	100	0.3	0.1	142

Carbothermal reduction	ZnS@N-dope d carbon	N	62.6	2	666	1000	0.021	1	147
Carbothermal reduction	RF-derived carbon & CNTs	N	40.5	3	600	200	0.158	0.2	140
Carbothermal reduction	Carbon	N (W/ CNT interlayer)	49	_	789	300	0.087	0.5	178
Carbothermal reduction	PVP-derived carbon	Y	55	3	520	200	0.18	1	174
Carbothermal reduction	CNTs & RGO	Y	55 – 60	1.0 – 1.5	975	300	0.037	0.2	106
Carbothermal reduction	CNTs & PVA-derived carbon	Y (W/ CNT interlayer)	-	1.86	520	220	0.05	1	109
Carbothermal reduction	Chitosan-deri ved carbon	Y (W/ carbon coating)	36	2	820	100	0.476	0.1	173
Carbothermal reduction	GO sponge	Y (w/ Al ₂ O ₃ coating)	58	1.2 – 1.5	668	1000	0.028	2	172
Reacting Li-Naph and S	PAN	N	37	0.42 – 1.06	484	250	0.038	0.14	112
Reacting Li-Naph and H_2S	Acetylene black	N	40	1.0	669	60	0.92	0.1	113
Reacting LiOH and H_2S	Carbon black	N	74	2.68	770	100	0.47	0.2	114
Reacting LiEt ₃ BH and S	Graphene	N	53	1.3	953	100	0.17	0.1	11
Reacting LiEt ₃ BH and S	carbon layer through CVD	N	88	1.1	972	100	0.24	0.2	115

			Journa.	i Pre-proc					
Reacting LiEt ₃ BH and S	GO & carbon layer through CVD	N	60	0.7 – 0.9	650	1500	0.046	2	118
Reacting LiEt ₃ BH and S	Graphene & carbon layer through CVD	N	60	1.1 – 1.3	993	100	0.24	0.2	116
Reacting LiEt ₃ BH and S	Ionic liquid-derived carbon	N	54	1.35 – 1.62	439.5	500	0.036	1	117
Reacting LiEt ₃ BH and S	GO & PAN-derived carbon	N	60	1.5	879	200	0.17	0.5	119
Reacting LiEt ₃ BH and S	Graphene aerogel	Y	69	3.66	838.5	100	0.55	0.1	120
Reacting LiEt ₃ BH and S	Li ₃ PS ₄ & graphene	Y	78.2	1.2	934.4	100	0.48	0.1	78
Reacting LiH and S	PAN-derived carbon	N	55.5	3-3.5	971	200	0.206	0.1	121
Reacting LiH and CS ₂	Porous carbon & CNTs	N	58.2	1.34 – 1.73	645	300	0.07	0.43	123
Reacting Li and CS ₂	Graphene	N	72	5	856	200	0.21	0.1	52
Reacting Li and S	Carbon	N	59.8	10	1014	100	0.06	0.1	77
Deeply discharging MoS_2	Electrolyte-de rived gel-like film	N	40	2-3	915	150	0.31	0.5	124
Deeply discharging MoS ₂	RGO & Electrolyte-de rived gel-like film	N	46.5	4.3 – 5.1	539	200	0.18	2	152

7. Li_2S -based lithium-metal-free cells

Due to the chronic safety concerns associated with the lithium metal anode, lithium metal-free anodes have been put forward to pair with Li₂S cathodes. This, in fact, is one of the significant advantages of Li₂S over elemental sulfur when used as the cathode in LSBs. Preliminary studies have been carried out on the Li₂S-based lithium-metal-free cells that use anodes such as graphite, ^{52, 81, 148, 185} Si, ^{9, 11, 111, 112, 124, 186-188} Sn, ^{10, 189} SnO₂, ⁷⁶ and Fe₃O₄. ^{27, 174} These anode materials have a theoretical capacity of 372, 4200, 994, 1491 and 924 mAh g⁻¹, respectively. The electrochemical performance of the Li₂S-based lithium-metal-free cells is summarized in Table 3 and Fig. 11.

Table 3. Electrochemical performance of Li₂S-based lithium-metal-free cells.

Cathode	Anode	Electrolyte	Average discharge voltage (V)	Initial capacity (mAh g ⁻¹)	Cycle number	Decay rate (% per cycle)	Current density (C)	Ref.
Li ₂ S-Ketjen black	Graphite	TRIDME/ LiTFSI/ HFE (1: 1: 4) (mol ratio)	1.7	487	50	1.1	0.1	185
Li ₂ S-Carbon nanotubes	Graphite	3M LiTFSI in 85/15 (v/v) DOL/DME	1.9	714	100	0.19	0.2	81
Li ₂ S@ Graphene nanocapsules	Graphite	1 M LiTFSI in 2/1 (v/v) D2/DOL	1.8	508	200	0.20	0.1	52
Li ₂ S-Micropo rous carbon	Graphite	1 M LiPF ₆ in 1/1 (v/v) EC/DEC	1.6	680	150	0.08	0.1	148
Li ₂ S	Silicon-Gra	1 M LiTFSI in 1/1 (v/v) DOL/DME w/ 0.5M LiNO ₃	1.8	540	70	0.7	0.2	188

Li ₂ S-Mesopor ous carbon	Silicon	1 M LiTFSI in 1/1 (v/v) DOL/DME	1.7	423	20	2.2	0.33	111
Li ₂ S-Graphen	Silicon	[Li(G4)][TFSA]/ HFE (1: 4) (mol ratio)	1.5	702	40	1.1	0.08	186
Li ₂ S-Graphen	Silicon	1 M LiTFSI in 1/1 (v/v) DOL/DME w/ LiNO ₃ & Li ₂ S _x	1.7	1000	10	1.0	0.05	11
Li ₂ S-Mesopor ous carbon	Prelithiated Si	LiOTf/TEGDME (1: 4) (mol ratio)	1.4	280	50	0.21	0.2	9
Li ₂ S-Poly (acrylonitrile)	Prelithiated Si	1 M LiPF ₆ in 1: 4: 5 (v/v/v) PC/EC/DEC	1.6	1026	50	0.39	0.14	112
Li ₂ S-Mo	Prelithiated Si	1 M LiPF ₆ in 1/1 (v/v) EC/DMC + 10% v/v FEC	1.4	788	150	0.32	0.2	124
Li ₂ S-Super C	Sn-Carbon	1 M LiPF ₆ in 1/1 (v/v) EC/DMC saturated by Li ₂ S in ZrO ₂ + PEO ₂₀ LiCF ₃ SO ₃	1.6	400	90	0.28	0.2	189
Li ₂ S-Carbon	Sn-Carbon	1 M LiPF ₆ in 1/1 (v/v) EC/DMC saturated by Li ₂ S in ZrO ₂ + PEO ₂₀ LiCF ₃ SO ₃	1.6	380	80	-0.42	0.2	10
Li ₂ S-Carboni zed wipe	SnO ₂ -Grap hene	1 M LiTFSI in 1/1 (v/v) DOL/DME w/ 1 wt% LiNO ₃ & 50 mM InI ₃	1.8	750	200	0.07	0.5	76
Li ₂ S@Carbon nanofiber	Fe ₃ O ₄ / Carbon nanosheets	1 M LiTFSI in 1/1 (v/v) DOL/DME w/ 2wt% LiNO ₃	1.9	576	50	0.80	0.2	174
Li ₂ S@MXene /Graphene	Fe ₃ O ₄ / Carbon nanosheets	1 M LiTFSI in 1/1 (v/v) DOL/DME w/ 2wt% LiNO ₃	1.6	560	50	0.44	0.2	27



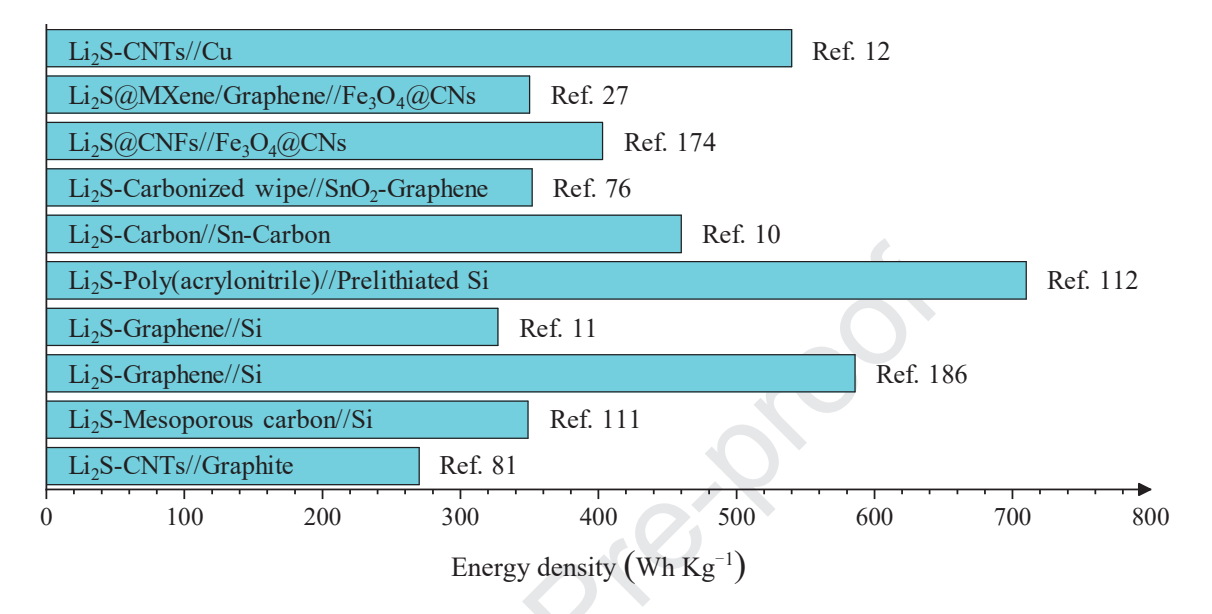


Fig. 11. Comparison of the reported energy density corresponding to different Li₂S-based full cells.

Even though some promising results have been achieved, many inherent problems related to the anode materials themselves remain to be solved before their practical applications. These include the low electronic conductivity of Si, SnO₂ and Fe₃O₄, and their huge volume change during charging/discharging, as summarized in Table 4. These anodes usually suffer from mechanical degradation, lithium loss and continuous electrolyte consumption due to instability of their SEI, their same problems used in either LIBs or LSBs. The only exception is graphite, but it is not a suitable candidate for LSBs due to its low specific capacity. A variety of strategies, such as nanostructuring and compositing the anode materials with electronically or/and ionically conductive matrixes, have been proposed to ameliorate the

problems associated with those large capacity anode materials. For example, Si nanowires can accommodate the large volume expansion upon lithium insertion, and good electronic contact and conduction could be retained. The compositing of Si or Sn with carbon can alleviate their poor electronic conductivity or volume expansion. It is a social to the problems associated with those large capacity anode materials. For example, Si nanowires can accommodate the large volume expansion upon lithium insertion, and good electronic contact and conduction could be retained.

Nevertheless, when these anodes are paired with Li₂S cathodes, several issues unique in LSBs will arise. The electrolyte, as the Li⁺ transport path connecting the cathode and the anode, should match both of them. Lithium loss due to side reactions might also arise.

Table 4. Comparison of different anodes applied in Li₂S-based LSBs.

Item	Graphite	Si	Sn	SnO_2	Fe ₃ O ₄
Specific capacity (mAh g ⁻¹)	372	4200	994	1491	924
Electronic conductivity at $25 \square (S m^{-1})$	8.4 × 10 ⁴	5 × 10 ⁻⁴	9.2×10^{6}	1.0×10^{-6}	4.4×10^{-1}
Volume expansion (%)	13	400	358	300	93

7.1 Electrolytes

Other than the cathode and the anode, the electrolyte, also plays a vital role in determining the LSB performance. The selected electrolyte, consisting of solvents, lithium salts, and additives, must be compatible with both electrodes. Currently, there have been no studies suggesting special lithium salts needed for Li₂S-based lithium-metal-free cells. As such, this section focuses only on solvents and additives.

7.1.1 Solvents

The commonly used ether-based electrolyte in lithium-metal based LSBs, which contains LiTFSI in 1, 3-dioxolane (DOL)/ DME and LiNO₃ additives will not work properly in Li₂S//graphite cells. Such an electrolyte can destroy the graphite structure because of the co-intercalation of solvent. ¹⁹⁵ An improved electrolyte with a high ratio of DOL to DME would generate a thin and uniform polymeric layer on graphite, thereby effectively reducing the irreversible capacity loss associated with the instability of SEI. ⁸¹ With DOL-rich electrolyte simultaneously appropriate for the Li₂S cathode and the graphite anode, Li₂S//graphite cells delivered a high capacity of 714 mAh g⁻¹ (based on Li₂S mass) at 0.2 C. ⁸¹ Wu et al. developed a novel electrolyte (triethyleneglycol dimethylether, LiTFSI and hydrofluoroether with a molar ratio of 1: 1: 4) matching well with both Li₂S and graphite, in which the Li₂S cathodes showed a high specific capacity around 1000 mAh g⁻¹ and a Coulombic efficiency around 95 % at 0.2 C when paired with a graphite anode. ¹⁸⁵

Si anodes demonstrate best performance in carbonate-based electrolytes, in which sulfur cathodes, however, fail to operate due to the nucleophilic addition or substitution reaction between polysulfide species and electrolyte components. On the other hand, Si anodes present poor performance in ether-based electrolytes. Even though, high-performance Li₂S//Si cells have been preliminary demonstrated using carbonate-based electrolytes, where the sulfur species are physically confined or chemically bonded in the host material and the generation of dissolved Li₂S_x is circumvented.

As for solid-state batteries, lithium metal anodes tend to react with almost all of the inorganic solid electrolytes that possess high ionic conductivity at room temperature, causing unstable interfaces. 197, 198 Nevertheless, the harmonious coexistence of Li₂S cathodes and Si

anodes with Li₇P₃S₁₁ opens a new avenue for developing all solid-state LSBs. ¹⁸⁷

Other solvents have also been applied in Li₂S-based lithium-metal-free cells, such as partially fluorinated solvent 1,1,2,2-tetrafluoro-3-(1,1,2,2-tetrafluoroethoxy)-propane (D2) and DOL, and tetraethylene glicole dymethylether (TEGDME).^{9, 52} Along with progress in Li₂S-based cathodes, more solvents compatible with both Li₂S cathode and lithium-metal-free anode are expected to be developed.

7.1.2 Additives

The function of additives in Li₂S-based LSBs could be categorized into either facilitating the Li₂S oxidation or promoting the formation of a stable SEI film. Both functions are crucial to the electrochemical performance of Li₂S-based LSBs.

As discussed in Section 2.2.1, the initial charging barrier could be effectively reduced by adopting additives in the electrolytes, whose identical function should also exist when a lithium-metal-free anode is used, but their effects on the anodes and the overall cell performance should be evaluated. Such studies are yet sparse.

A stable SEI film on the anode is critical for the operation of LSBs. In the conventional Li₂S//Li cells, the reaction between lithium polysulfides and lithium foil will lead to loss of active materials and lithium foil coated by poorly electronically conductive Li₂S and Li₂S₂, resulting in low utilization of active materials and unstable cycling performance. LiNO₃ was added as a co-salt or additive in the electrolyte to promote the formation of a stable passivation film on the lithium anode in order to suppress the growth of lithium dendrite and the redox shuttling of Li₂S_x. ¹⁹⁹ Other additives to facilitate the formation of SEI films on

lithium foils include Li_2S_x , ²⁰⁰ lithium bis (oxalate) borate (LiBOB), ²⁰¹ and Biphenyl-4,4'-dithiol (BPD), ²⁰² etc.

When lithium metal is substituted with Si or SnO₂, the reaction between Li⁺ in Si or SnO₂ anodes and lithium polysulfides still exist.^{203, 204} And even worse, compared with lithium anodes, the prelithiated anodes are more reactive with lithium polysulfides, as there are more Li⁺ exposed to the electrolyte when nanostructured anodes are used.²⁰³ Although a variety of additives have been investigated in lithium-metal based LSBs to alleviate the shuttle effect, such is not yet the case for other anodes based cells. Although LiNO₃ and LiNO₃/Li₂S_x were adopted as additives in Li₂S-based lithium-metal-free cells,^{11, 27, 174, 188} their functions were not investigated. In a novel Li₂S-based lithium-metal-free cell (Li₂S//Cu), Nanda et al. demonstrated the presence of lithium polysulfides would facilitate the reversible plating and stripping of lithium.¹² In Li₂S//Cu cells, dissolved lithium polysulfides play a positive role in mediating the lithium deposition process by forming protective Li₂S and Li₂S₂ regions on the deposited lithium. Li₂S//Cu cells thus demonstrated Coulombic efficiencies over 96%, much higher than that of LiFePO₄//Cu full cells (68.3%).¹²

Liu et al. established a passivation layer (Li-In alloy) on the surface of the SnO_2 anode by using InI_3 as an additive in the electrolyte, which protected the anode from corrosion by polysulfides and allows for facile Li^+ transport. The $Li_2S//SnO_2$ cells exhibited excellent rate capability with 675 mAh g^{-1} delivered at 1.5 C, and stable cycling performance with 647 mAh g^{-1} retained after 200 cycles at 0.5 C. Therefore, a SEI film formed on the anodes using additives would provide a promising strategy for alleviating the shuttle effect of lithium polysulfides.

In general, the reports on the solvents and additives applied in Li_2S based lithium-metal-free cells are relatively few, and more studies are needed, either to confirm the functions of those commonly used solvents and additives or develop new ones.

7.2 Compensating the lithium loss

The SEI formation and the partly irreversible lithiation will result in a considerable lithium loss. ^{52, 81, 112, 186} In cells composed of Li₂S cathodes and lithium-metal-free anodes, Li₂S cathodes are the sole source of lithium and lithium loss will significantly impact the cell performance. For example, compared with Li₂S//Si cells, Li₂S//graphite cells demonstrated a smaller capacity fading because the graphite electrode underwent a much smaller volume change (10%) during lithium intercalation and lithium loss was suppressed. ¹⁸⁶

Several strategies have been proposed to ameliorate the detrimental effect of lithium loss in lithium-metal-free cells, either by adding sacrificial lithium to the cathode or through anode prelithiation. For example, excess lithium metal powder can be added for Li₂S preparation, which will serve as extra lithium source. Si electrodes can be prelithiated before assembled into a cell using electrochemical method. Specifically, the Si electrode is paired with a lithium foil and then discharged. After that, the lithiated Si electrode is assembled with a Li₂S cathode into a cell. In contrast to electrochemical prelithiation, Shen et al. developed a facile chemical prelithiation strategy to achieve lithiated Si electrode. Prelithiation was conducted by reacting Si electrode with Li-Naph at room temperature, and the lithiation degree could be simply controlled by the reaction time.

The progress made on prelithiation technology will address the capacity degradation

issues associated with lithium loss.

8. Summary and future works

Towards developing practical LSBs, Li₂S-based cathodes have been investigated in recent years and strategies to fabricate the electrode with much improved performance have been reported. With its electronic and ionic insulation nature, the size, morphology, and crystallinity of Li₂S particles play critical roles in determining its initial activation and the subsequent cathode performance. Several approaches to prepare nanoscale Li₂S particles via physical or chemical routes have been demonstrated, although their cost, production efficiency, and safety issues are yet to be evaluated. To prevent the nanoparticle aggregation and particularly to diminish the polysulfide shuttling effects, encapsulation of preformed Li₂S nanoparticles by materials with excellent electronic conductivity or Li⁺ conductivity is necessary, which has greatly enhanced the electrochemical performance of Li₂S cathodes. Simultaneously synthesizing and encapsulating Li₂S nanoparticles in one step is a preferable strategy in solving the aggregation issues of nanoparticles. The high melting temperature of Li₂S opens avenues of high-temperature processing, and several approaches have been reported to simultaneously prepare and encapsulate these Li₂S nanoparticles. As one more step, Li₂S-based free-standing structures directly used as cathodes are also attracting interests and steady progress is being made. A coating or an interlayer that can be directly formed on the electrode has been found to be effective in alleviating the loss of active materials and reducing the shuttling effects. In the cell level, studies on electrolytes and lithium-metal-free anodes for building high-performance Li₂S full cells are also being conducted.

Despite great progress being made, there is still plenty of room in the fundamental study of the electrochemical processes and the practical development of the electrode nanostructures and the whole cell construction toward a practical LSB technology. We consider following are some of the research opportunities that deserve to be pursued:

- 1) As there is still controversy on the detail steps of the first charging process, fundamental studies are called for unequivocally clarifying the mechanism of Li₂S activation. This understanding could provide critical guidance for the rational design of Li₂S cathode structure and the selection of electrolyte in order to reduce the charging overpotential and elevate utilization of the active material.
- 2) Other than engineering the Li₂S particles and developing host materials, modifying the electrolyte, especially adding RMs, is an effective and facile method to reduce the activation voltage. The study on this aspect is still in the early stage, and more effective additives might be developed through calculation-based material design and experimental demonstration.
- 3) Many studies on effects of Li₂S particle size have been reported; however, the particle morphology and crystallinity, both of which have demonstrated similar effects as the particle size on Li₂S cathode performance, were rarely investigated. Efforts on morphology and crystallinity engineering of Li₂S particles, in addition to their dimension, provide more degrees of freedom to further promote Li₂S cathode performance.
- 4) The high-temperature stability of Li₂S opens many new avenues for its encapsulation, including the selection of coating materials. Since Li₂S has poor both electronic and lithium ionic conductivities, a mixed ionic-electronic conductor as the encapsulation coating has potential to synergistically enhance the Li₂S cathode performance. Studies along this

direction, particularly those that also combine with solid-state electrolytes, might lead to novel and even breakthrough works. It must be emphasized that in order to surpass the energy density of LIBs, the Li₂S content and loading in the cathode must be largely increased than many reports. Toward this end, more delicate encapsulation strategies are required to tailor the encapsulation layer thickness, surface area, pore volume, etc.

- 5) With mechanism understanding and optimization on different aspects, a holistic strategy is called for to design the Li₂S cathode, including but not limited to the size, morphology, crystallinity, and the selection of coating materials, to enhance the electronic and Li⁺ conductivities, alleviate the volume expansion, strongly immobilize sulfur species, and catalyze their redox reaction.
- 6) To develop practical Li₂S-based LSBs, anode materials other than lithium metal should also be investigated to couple with Li₂S cathodes. This requires to solve the issues of poor electronic conductivity and large volume expansion associated with the lithium metal-free anodes. New electrolytes that simultaneously match Li₂S cathodes and lithium metal-free anodes are desired to be developed. The strategies to protect Li₂S_x from reaction with anodes are urgently needed. Techniques for compensating the lithium loss should also be developed.

Acknowledgements

The authors would like to appreciate Zhejiang Provincial Natural Science Foundation of China for providing financial support (Grant No. LY19E020011). Z.F acknowledges support from National Science Foundation (1931737) for the work at Texas Tech University.

References

- M. Zhao, H.J. Peng, Z.W. Zhang, B.Q. Li, X. Chen, J. Xie, X. Chen, J.Y. Wei, Q. Zhang,
 J.Q. Huang, *Angew. Chem. Int. Ed.* 2019, 58, 3779-3783.
- F. Pei, A. Fu, W. Ye, J. Peng, X. Fang, M.S. Wang, N. Zheng, ACS Nano 2019, 13, 8337-8346.
- 3. W. Xue, Z. Shi, L. Suo, C. Wang, Z. Wang, H. Wang, K.P. So, A. Maurano, D. Yu, Y. Chen, L. Qie, Z. Zhu, G. Xu, J. Kong, J. Li, *Nat. Energy* **2019**, *4*, 374-382.
- 4. S. Li, T. Mou, G. Ren, J. Warzywoda, Z. Wei, B. Wang, Z. Fan, *J. Mater. Chem. A* **2017**, 5, 1650-1657.
- 5. G. Ren, S. Li, Z.X. Fan, J. Warzywoda, Z. Fan, J. Mater. Chem. A 2016, 4, 16507-16515.
- S. Li, T. Mou, G. Ren, J. Warzywoda, B. Wang, Z. Fan, ACS Energy Lett. 2016, 1, 481-489.
- 7. C. Du, J. Wu, P. Yang, S. Li, K. Song, Electrochim. Acta 2018, 295, 1067-1074.
- 8. B.D. McCloskey, J. Phys. Chem. Lett. **2015**, 6, 4581-4588.
- 9. M. Agostini, J. Hassoun, J. Liu, M. Jeong, H. Nara, T. Momma, T. Osaka, Y.K. Sun, B. Scrosati, *ACS Appl. Mater. Inter.* **2014**, *6*, 10924-10928.
- 10. J. Hassoun, Y.K. Sun, B. Scrosati, J. Power Sources 2011, 196, 343-348.
- 11. K. Zhang, L. Wang, Z. Hu, F. Cheng, J. Chen, Sci. Rep. 2014, 4, 6467.
- 12. S. Nanda, A. Gupta, A. Manthiram, *Adv. Energy Mater.* **2018**, *8*, 1801556.
- 13. S. Lorger, R.E. Usiskin, J. Maier, Adv. Funct. Mater. 2019, 29, 1807688.
- S. Li, J. Jiang, Z. Dong, J. Wu, Z. Cheng, H. Zhu, Z. Fan, Y. Wang, D. Leng, *Micropor. Mesopor. Mater.* 2020, 293, 109822.
- 15. S. Jeong, D. Bresser, D. Buchholz, M. Winter, S. Passerini, *J. Power Sources* **2013**, *235*, 220-225.
- Y. Kim, H. Han, Y. Noh, J. Bae, M.H. Ham, W.B. Kim, ChemSusChem 2019, 12, 824-829.
- 17. Z. Seh, H. Wang, N. Liu, G. Zheng, W. Li, H. Yao, Y. Cui, *Chem. Sci.* **2014**, *5*, 1396-1400.
- 18. X. Wang, X. Bi, S. Wang, Y. Zhang, H. Du, J. Lu, ACS Appl. Mater. Inter. 2018, 10,

- 16552-16560.
- 19. F.X. Wu, J.T. Lee, F.F. Fan, N. Nitta, H. Kim, T. Zhu, G. Yushin, *Adv. Mater.* **2015**, *27*, 5579.
- 20. L. Chen, Y. Liu, N. Dietz-Rago, L.L. Shaw, Nanoscale 2015, 7, 18071-18080.
- T. Takeuchi, H. Sakaebe, H. Kageyama, H. Senoh, T. Sakai, K. Tatsumi, *J. Power Sources* 2010, 195, 2928-2934.
- 22. Y. Yang, G. Zheng, S. Misra, J. Nelson, M.F. Toney, Y. Cui, *J. Am. Chem. Soc.* **2012**, *134*, 15387-15394.
- 23. S.H. Chung, P. Han, C.H. Chang, A. Manthiram, Adv. Energy Mater. 2017, 7, 1700537.
- D. Wang, X. Xia, Y. Wang, D. Xie, Y. Zhong, J. Wu, X. Wang, J. Tu, Chem. Eur. J. 2017,
 23, 11169-11174.
- 25. J. He, Y. Chen, W. Lv, K. Wen, C. Xu, W. Zhang, W. Qin, W. He, *ACS Energy Lett.* **2016**, *1*, 820-826.
- C. Wang, X. Wang, Y. Yang, A. Kushima, J. Chen, Y. Huang, J. Li, *Nano Lett.* 2015, 15, 1796-1802.
- 27. Z. Wang, N. Zhang, M. Yu, J. Liu, S. Wang, J. Qiu, J. Energy Chem. 2019, 37, 183-191.
- 28. M.A. Pope, I.A. Aksay, Adv. Energy Mater. 2015, 5, 1500124.
- 29. L. Zhen, Y. Huang, L. Yuan, Z. Hao, Y. Huang, Carbon 2015, 92, 41-63.
- 30. A. Rosenman, E. Markevich, G. Salitra, D. Aurbach, A. Garsuch, F.F. Chesneau, *Adv. Energy Mater.* **2015**, *5*, 1500212.
- 31. B. Dominic, P. Stefano, S. Bruno, Chem. Commun. 2013, 49, 10545-10562.
- 32. X. Chen, T. Hou, K.A. Persson, Q. Zhang, *Mater. Today* **2019**, *22*, 142-158.
- 33. H. Yuan, J.Q. Huang, H.J. Peng, M.M. Titirici, R. Xiang, R. Chen, Q. Liu, Q. Zhang, *Adv. Energy Mater.* **2018**, *8*, 1802107.
- 34. Q. Zhang, F. Li, J.Q. Huang, H. Li. Adv. Funct. Mater. 2018, 28, 1804589.
- 35. M. Wild, L. O'Neill, T. Zhang, R. Purkayastha, G. Minton, M. Marinescu, G.J. Offer, *Energ. Environ. Sci.* **2015**, *8*, 3477-3494.
- 36. N. Deng, W. Kang, Y. Liu, J. Ju, D. Wu, L. Li, B. Hassan, B. Cheng, *J. Power Sources* **2016**, *331*, 132-155.

- H. Yuan, T. Liu, Y. Liu, J. Nai, Y. Wang, W. Zhang, X. Tao, Chem. Sci. 2019, 10, 7484-7495.
- 38. Y. Wang, E. Sahadeo, G. Rubloff, C.F. Lin, S.B. Lee, *J. Mater. Sci.* **2019**, *54*, 3671-3693.
- 39. H. Zhao, N. Deng, J. Yan, W. Kang, J. Ju, Y. Ruan, X. Wang, X. Zhuang, Q. Li, B. Cheng, Chem. Eng. J. 2018, 347, 343-365.
- 40. S. Li, B. Jin, X. Zhai, H. Li, Q. Jiang, ChemistrySelect 2018, 3, 2245-2260.
- 41. B. Yan, X. Li, Z. Bai, X. Song, D. Xiong, M. Zhao, D. Li, S. Lu, *J. Power Sources* **2017**, *338*, 34-48.
- 42. R. Fang, S. Zhao, Z. Sun, W. Wang, H.M. Cheng, F. Li, Adv. Mater. 2017, 29, 1606823.
- 43. M. Barghamadi, A.S. Best, A.I. Bhatt, A.F. Hollenkamp, M. Musameh, R.J. Rees, T. Ruther, *Energ. Environ. Sci.* **2014**, *7*, 3902-3920.
- 44. A. Manthiram, Y. Fu, Y.S. Su, Acc. Chem. Res. 2013, 46, 1125-1134.
- 45. J. Scheers, S. Fantini, P. Johansson, J. Power Sources 2014, 255, 204-218.
- 46. M.R. Kaiser, Z. Han, J. Liang, S.X. Dou, J.Z. Wang, *Energy Storage Mater.* **2019**, *19*, 1-15.
- 47. S.K. Lee, J.L. Yun, Y.K. Sun, J. Power Sources 2016, 323, 174-188.
- 48. Y. Son, J.S. Lee, Y. Son, J.H. Jang, J. Cho, Adv. Energy Mater. 2015, 5, 1500110.
- 49. D. Su, D. Zhou, C. Wang, G. Wang, Adv. Funct. Mater. 2018, 28, 1870273.
- 50. S. Waluś, C. Barchasz, R. Bouchet, J.F. Martin, J.C. Leprêtre, F. Alloin, *Electrochim. Acta.* 2015, 180, 178-186.
- 51. K. Cai, M.K. Song, E.J. Cairns, Y.J.N.L. Zhang, Nano Lett. 2012, 12, 6474-6479.
- 52. G. Tan, R. Xu, Z. Xing, Y. Yuan, J. Lu, J. Wen, C. Liu, L. Ma, C. Zhan, Q. Liu, T. Wu, Z. Jian, R. Shahbazian-Yassar, Y. Ren, D.J. Miller, L.A. Curtiss, X. Ji, K. Amine, *Nat. Energy* **2017**, *2*, 17090.
- 53. L. Zhang, D. Sun, J. Feng, E.J. Cairns, J.H. Guo, *Nano Lett.* **2017**, *17*, 5084-5091.
- 54. A. Vizintin, L. Chabanne, E. Tchernychova, I. Arčon, L. Stievano, G. Aquilanti, M. Antonietti, T.P. Fellinger, R. Dominko, *J. Power Sources* **2017**, *344*, 208-217.
- 55. Y. Gorlin, M. Patel, A. Freiberg, Q. He, M. Piana, M. Tromp, H. Gasteiger, J. Electrochem. Soc. 2016, 163, A930-A939.

- 56. L. Wang, Y. Wang, Y.Y. Xia, Energ. Environ. Sci. 2015, 8, 1551-1558.
- 57. Z. Liu, H. Deng, W. Hu, F. Gao, S. Zhang, P.B. Balbuena, P.P. Mukherjee, *Phys. Chem. Chem. Phys.* **2018**, *20*, 11713-11721.
- 58. B. Kang, Y.J. Jung, Phys. Chem. Chem. Phys. 2016, 18, 21500-21507.
- 59. J. Koh, M.S. Park, E.H. Kim, B. Jeong, S. Kim, K. Kim, J.G. Kim, Y. Kim, Y. Jung, *J. Electrochem. Soc.* **2014**, *161*, A2133-A2137.
- 60. K.R. Ryan, L. Trahey, B.J. Ingram, A.K. Burrell, *J. Phys. Chem. C.* **2012**, *116*, 19724-19728.
- 61. F. Ye, M. Liu, X. Yan, J. Li, Z. Pan, H. Li, Y. Zhang, Small 2018, 14, 1703871.
- 62. H. Pan, K.S. Han, V. Murugesan, J. Xiao, R. Cao, J. Chen, J. Zhang, K.T. Mueller, Y. Shao, J. Liu, *ACS Appl. Mater. Inter.* **2016**, *9*, 4290-4295.
- 63. X. Liang, J. Yun, K. Xu, P. Shi, Y. Sun, C. Chen, H. Xiang, *Chem. Commun.* **2019**, *55*, 10088-10091.
- 64. F. Wu, J.T. Lee, N. Nitta, H. Kim, O. Borodin, G. Yushin, Adv. Mater. 2015, 27, 101-108.
- 65. C. Zu, M. Klein, A. Manthiram, J. Phys. Chem. Lett. 2014, 5, 3986-3991.
- 66. H.D. Lim, B. Lee, Y. Zheng, J. Hong, J. Kim, H. Gwon, Y. Ko, M. Lee, K. Cho, K. Kang, *Nat. Energy* **2016**, *1*, 16066.
- 67. Z. Liang, Y.C. Lu, J. Am. Chem. Soc. 2016, 138, 7574-7583.
- 68. D. Kundu, R. Black, B. Adams, L.F. Nazar, ACS Central Sci. 2015, 1, 510-515.
- 69. Y. Tsao, M. Lee, E.C. Miller, G. Gao, J. Park, S. Chen, T. Katsumata, H. Tran, L.W. Wang, M.F. Toney, Y. Cui, Z. Bao, *Joule* **2019**, *3*, 872-884.
- H. Chu, H. Noh, Y.J. Kim, S. Yuk, J.H. Lee, J. Lee, H. Kwack, Y. Kim, D.K. Yang, H.T. Kim, Nat. Commun. 2019, 10, 188.
- 71. H.J. Peng, J.Q. Huang, X.Y. Liu, X.B. Cheng, W.T. Xu, C.Z. Zhao, F. Wei, Q. Zhang, J. Am. Chem. Soc. **2017**, 139, 8458-8466.
- 72. M. Kohl, J. Brückner, I. Bauer, H. Althues, S. Kaskel, *J. Mater. Chem. A* **2015**, *3*, 16307-16312.
- 73. R. Xu, X. Zhang, C. Yu, Y. Ren, J.C.M. Li, I. Belharouak, *ChemSusChem* **2014**, 7, 2457-2460.

- 74. P.D. Frischmann, L.C.H. Gerber, S.E. Doris, E.Y. Tsai, F.Y. Fan, X. Qu, A. Jain, K.A. Persson, Y.M. Chiang, B.A. Helms, *Chem. Mater.* **2015**, *27*, 6765-6770.
- 75. S. Meini, R. Elazari, A. Rosenman, A. Garsuch, D. Aurbach, *J. Phys. Chem. Lett.* **2014**, *5*, 915-918.
- 76. M. Liu, Y.X. Ren, H.R. Jiang, C. Luo, F.Y. Kang, T.S. Zhao, *Nano Energy* **2017**, *40*, 240-247.
- 77. C. Chen, D. Li, L. Gao, P.P.R.M.L. Harks, R.A. Eichel, P.H.L. Notten, *J. Mater. Chem. A* **2017**, *5*, 1428-1433.
- 78. Z. Jiao, L. Chen, J. Si, C. Xu, Y. Jiang, Y. Zhu, Y. Yang, B. Zhao, *J. Power Sources* **2017**, *353*, 167-175.
- 79. Z. Lin, Z. Liu, N.J. Dudney, C. Liang, ACS Nano 2013, 7, 2829-2833.
- 80. C. Xiong, T.S. Zhao, Y.X. Ren, H.R. Jiang, X.L. Zhou, *Electrochim. Acta.* **2019**, *296*, 954-963.
- 81. F.M. Ye, H. Noh, H. Lee, H.T. Kim, Adv. Sci. 2018, 5, 1800139.
- 82. X.B. Meng, D.J. Comstock, T.T. Fister, J.W. Elam, ACS Nano 2014, 8, 10963-10972.
- 83. H. Noh, J. Song, J.K. Park, H.T. Kim, J. Power Sources 2015, 293, 329-335.
- 84. L. Lodovico, S.M. Hosseini, A. Varzi, S. Passerini, Energy Technology 2019, 7, 1801013.
- 85. D.H. Wang, X.H. Xia, D. Xie, X.Q. Niu, X. Ge, C.D. Gu, X.L. Wang, J.P. Tu, *J. Power Sources* **2015**, *299*, 293-300.
- 86. D.H. Wang, D. Xie, T. Yang, Y. Zhong, X.L. Wang, X.H. Xia, C.D. Gu, J.P. Tu, *J. Power Sources* **2016**, *313*, 233-239.
- 87. G. Zhou, H. Tian, Y. Jin, X. Tao, B. Liu, R. Zhang, Z.W. Seh, D. Zhuo, Y. Liu, J. Sun, J. Zhao, C. Zu, D.S. Wu, Q. Zhang, Y. Cui, *Proc. Natl. Acad. Sci.* **2017**, *114*, 840-845.
- 88. Q.Q. Fan, B.H. Li, Y.B. Si, Y.Z. Fu, Chem. Commun. 2019, 55, 7655-7658.
- 89. H.D. Yuan, X.L. Chen, G.M. Zhou, W.K. Zhang, J.M. Luo, H. Huang, Y.P. Gan, C. Liang, Y. Xia, J. Zhang, J.G. Wang, X.Y. Tao, *ACS Energy Lett.* **2017**, *2*, 1711-1719.
- 90. R. Demir-Cakan, J. Power Sources **2015**, 282, 437-443.
- 91. F. Wu, A. Magasinski, G. Yushin, J. Mater. Chem. A. 2014, 2, 6064-6070.
- 92. M.R. Kaiser, X. Liang, H.K. Liu, S.X. Dou, J.Z. Wang, Carbon 2016, 103, 163-171.
- 93. L. Chen, Y. Liu, M. Ashuri, C. Liu, L.L. Shaw, J. Mater. Chem. A 2014, 2, 18026-18032.

- 94. L. Chen, Y. Liu, F. Zhang, C. Liu, L.L. Shaw, ACS Appl. Mater. Inter. 2015, 7, 25748-25756.
- 95. T. Yang, X. Wang, D. Wang, S. Li, D. Xie, X. Zhang, X. Xia, J. Tu, *J. Mater. Chem. A* **2016**, *4*, 16653-16660.
- 96. J. He, Y. Chen, W. Lv, K. Wen, C. Xu, W. Zhang, Y. Li, W. Qin, W. He, ACS Nano 2016, 10, 10981-10987.
- 97. D. Wang, X. Dong, X. Xia, X. Zhang, W. Tang, Z. Yu, J. Wu, X. Wang, J. Tu, *J. Mater. Chem. A* **2017**, *5*, 19358-19363.
- 98. M. Wu, Y. Cui, Y. Fu, ACS Appl. Mater. Inter. 2015, 7, 21479-21486.
- 99. C. Hu, H. Chen, Y. Xie, L. Fang, J. Fang, J. Xu, H. Zhao, J. Zhang, *J. Mater. Chem. A* **2016**, *4*, 18284-18288.
- 100. P. Strubel, H. Althues, S. Kaskel, *ChemNanoMat* **2016**, 2, 656-659.
- 101. F. Ye, Y. Hou, M. Liu, W. Li, X. Yang, Y. Qiu, L. Zhou, H. Li, Y. Xu, Y. Zhang, *Nanoscale* **2015**, *7*, 9472-9476.
- 102. K. Han, J. Shen, C.M. Hayner, H. Ye, M.C. Kung, H.H. Kung, *J. Power Sources* **2014**, *251*, 331-337.
- 103. Y. Qiu, G. Rong, J. Yang, G. Li, S. Ma, X. Wang, Z. Pan, Y. Hou, M. Liu, F. Ye, *Adv. Energy Mater.* **2016**, *5*, 1501369.
- 104. Y. Peng, Y. Zhang, Z. Wen, Y. Wang, Z. Chen, B.J. Hwang, J.B. Zhao, *Chem. Eng. J.* **2018**, *346*, 57-64.
- 105. W. Ning, N. Zhao, C. Shi, E. Liu, C. He, H. Fang, L. Ma, *Electrochim. Acta* **2017**, *256*, 348-356.
- 106. Y. Chen, S. Lu, J. Zhou, W. Qin, X. Wu, Adv. Funct. Mater. 2017, 27, 1700987.
- 107. J. Liu, H. Nara, T. Yokoshima, T. Momma, T. Osaka, *Electrochim. Acta* 2015, 183, 70-77.
- 108. Z. Li, S. Zhang, S. Terada, X. Ma, K. Ikeda, Y. Kamei, C. Zhang, K. Dokko, M. Watanabe, *ACS Appl. Mater. Inter.* **2016**, *8*, 16053-16062.
- 109. F. Ye, H. Noh, J. Lee, H. Lee, H.T. Kim, J. Mater. Chem. A 2018, 6, 6617-6624.
- 110. Z. Li, S. Zhang, C. Zhang, K. Ueno, T. Yasuda, R. Tatara, K. Dokko, M. Watanabe,

- Nanoscale 2015, 7, 14385-14392.
- 111. Y. Yang, M.T. Mcdowell, A. Jackson, J.J. Cha, S.S. Hong, Y. Cui, *Nano Lett.* **2010**, *10*, 1486.
- 112.Y. Shen, J. Zhang, Y. Pu, H. Wang, B. Wang, J. Qian, Y. Cao, F. Zhong, X. Ai, H. Yang, *ACS Energy Lett.* **2019**, *4*, 1717-1724.
- 113. X. Li, C.A. Wolden, C. Ban, Y. Yang, ACS Appl. Mater. Inter. 2015, 7, 28444-28451.
- 114. C.B. Dressel, H. Jha, A.M. Eberle, H.A. Gasteiger, T.F. Fässler, *J. Power Sources* **2016**, *307*, 844-848.
- 115. C. Nan, Z. Lin, H. Liao, M.K. Song, Y. Li, E.J. Cairns, *J. Am. Chem. Soc.* **2014**, *136*, 4659-4663.
- 116. D. Sun, Y. Hwa, Y. Shen, Y. Huang, E. Cairns, *Nano Energy* **2016**, *26*, 524-532.
- 117. L. Suo, Y. Zhu, F. Han, G. Tao, L. Chao, X. Fan, Y.S. Hu, C. Wang, *Nano Energy* **2015**, *13*, 467-473.
- 118. Y. Hwa, J. Zhao, E. Cairns, Nano Lett. 2015, 15, 3479-3486.
- 119. L. Zhan, C. Nan, Y. Ye, J. Guo, J. Zhu, E. Cairns, *Nano Energy* **2014**, *9*, 408-416.
- 120. Z.X. Wang, C.X. Xu, L. Chen, J. Si, W.R. Li, S.S. Huang, Y. Jiang, Z.W. Chen, B. Zhao, *Electrochim. Acta* **2019**, *312*, 282-290.
- 121. X. Li, M. Gao, W. Du, B. Ni, Y. Wu, Y. Liu, C. Shang, Z. Guo, H. Pan, *J. Mater. Chem. A* **2017**, *5*, 6471-6482.
- 122. H. Yan, H. Wang, D. Wang, X. Li, Z. Gong, Y. Yang, Nano Lett. 2019, 19, 3280-3287.
- 123. L. Sheng, X. Yang, L. Chu, Y. Gan, H. Hui, J. Zhang, X. Tao, S. Wei, W. Han, W.K. Zhang, *J. Mater. Chem. A* **2018**, *6*, 9906-9914.
- 124. J. Balach, T. Jaumann, L. Giebeler, Energy Storage Mater. 2017, 8, 209-216.
- 125. S. Liang, C. Liang, Y. Xia, H. Xu, H. Huang, X. Tao, Y. Gan, W. Zhang, *J. Power Sources* **2016**, *306*, 200-207.
- 126. F.D. Han, J. Yue, X. Fan, T. Gao, C. Luo, Z. Ma, L. Suo, C. Wang, *Nano Lett.* **2016**, *16*, 4521-4527.
- 127. D. Sun, Y. Hwa, L. Zhang, J. Xiang, J. Guo, Y. Huang, E.J. Cairns, *Nano Energy* 2019, 64, 103891.

- 128. Z.W. Seh, J.H. Yu, W. Li, P.C. Hsu, H. Wang, Y. Sun, H. Yao, Q. Zhang, Y. Cui, *Nat. Commun.* **2014**, *5*, 5017.
- 129. Z. Yuan, H.J. Peng, T.Z. Hou, J.Q. Huang, C.M. Chen, D.W. Wang, X.B. Cheng, F. Wei,Q. Zhang, *Nano Lett.* 2016, *16*, 519-527.
- 130. J. He, A. Manthiram, *Energy Storage Mater.* **2019**, *20*, 55-70.
- 131. M.J. Klein, A. Dolocan, C. Zu, A. Manthiram, *Adv. Energy Mater.* **2017**, *7*, 1701122.
- 132. J. He, Y. Chen, A. Manthiram, *Adv. Energy Mater.* **2019**, *9*, 1900584.
- 133. C. Zheng, S.Z. Niu, W. Lv, G.M. Zhou, J. Li, S.X. Fan, Y.Q. Deng, Z.Z. Pan, B.H. Li, F.Y. Kang, Q.H. Yang, *Nano Energy* **2017**, *33*, 306-312.
- 134. G. Jiang, F. Xu, S. Yang, J. Wu, B. Wei, H. Wang, J. Power Sources 2018, 395, 77-84.
- 135. Y. Luo, N. Luo, W. Kong, H. Wu, K. Wang, S. Fan, W. Duan, J. Wang, *Small* **2018**, *14*, 1702853.
- 136. Q. Pang, J.T. Tang, H. Huang, X. Liang, C. Hart, K.C. Tam, L.F. Nazar, *Adv. Mater.* **2015**, *27*, 6021-6028.
- J. Liang, X. Li, Y. Zhao, L.V. Goncharova, G. Wang, K.R. Adair, C. Wang, R. Li, Y. Zhu,
 Y. Qian, L. Zhang, R. Yang, S. Lu, X. Sun, *Adv. Mater.* 2018, *30*, 1804684.
- 138. C. Luo, X. Ji, J. Chen, K.J. Gaskell, X. He, Y. Liang, J. Jiang, C. Wang, Angew. Chem. Int. Ed. 2018, 57, 8567-8571.
- 139. F. Wu, T.P. Pollard, E. Zhao, Y. Xiao, M. Olguin, O. Borodin, G. Yushin, *Energy Environ. Sci.* **2018**, *11*, 807-817.
- 140. X. Chen, L. Peng, L. Yuan, R. Zeng, J. Xiang, W. Chen, K. Yuan, J. Chen, Y. Huang, J. Xie, J. Energy Chem. 2019, 37, 111-116.
- 141. Z. Yang, J. Guo, S. Das, Y. Yu, Z. Zhou, H. Abruna, L. Archer, J. Mater. Chem. A 2013, 1, 1433-1440.
- 142. J. Zhang, Y. Shi, Y. Ding, L. Peng, W. Zhang, G. Yu, *Adv. Energy Mater.* **2017**, *7*, 1602876.
- 143. T.Z. Hou, W.T. Xu, X. Chen, H.J. Peng, J.Q. Huang, Q. Zhang, *Angew. Chem. Int. Ed.* **2017**, *129*, 8178-8182.
- 144. T.Z. Hou, X. Chen, H.J. Peng, J.Q. Huang, B.Q. Li, Q. Zhang, B. Li, Small 2016, 12,

- 3283-3291.
- 145. S. Li, J. Warzywoda, W. Shu, G. Ren, Z. Fan, Carbon 2017, 124, 212-218.
- 146. L. Qie, A. Manthiram, *Chem. Commun.* **2016**, *52*, 10964-10967.
- 147. M.L. Yu, S. Zhou, Z.Y. Wang, W. Pei, X.J. Liu, C. Liu, C.L. Yan, X.Y. Meng, S. Wang, J.J. Zhao, J.S. Qiu, Adv. Funct. Mater. 2019, 29, 1905986.
- 148. S.Y. Zheng, Y. Chen, Y.H. Xu, F. Yi, Y.J. Zhu, Y.H. Liu, J.H. Yang, C.S. Wang, *ACS Nano* **2013**, *7*, 10995-11003.
- 149. I.A. Shkrob, Y. Zhu, T.W. Marin, D. Abraham, J. Phys. Chem. C 2013, 117, 19255-19269.
- 150. H. Kumar, E. Detsi, D. Abraham, V. Shenoy, *Chem. Mater.* **2016**, *28*, 8930-8941.
- 151. Y.M. Sun, H.W. Lee, Z.W. Seh, G.Y. Zheng, J. Sun, Y.B. Li, Y. Cui, *Adv. Energy Mater.* **2016**, *6*, 1600154.
- 152. M. Zensich, T. Jaumann, G.M. Morales, L. Giebeler, C.A. Barbero, J. Balach, *Electrochim. Acta* **2019**, *296*, 243-250.
- 153. X.N. Li, J.W. Liang, W.H. Li, J. Luo, X. Li, X.F. Yang, Y.F. Hu, Q.F. Xiao, W.Q. Zhang, R.Y. Li, T.K. Sham, X.L. Sun, *Chem. Mater.* **2019**, *31*, 2002-2009.
- 154. T. Yim, M.S. Park, J.S. Yu, K.J. Kim, K.Y. Im, J.H. Kim, G. Jeong, Y.N. Jo, S.G. Woo, K.S. Kang, I. Lee, Y.J. Kim, *Electrochim. Acta* **2013**, *107*, 454-460.
- 155. S. Xin, L. Gu, N.H. Zhao, Y.X. Yin, L.J. Zhou, Y.G. Guo, L.J. Wan, *J. Am. Chem. Soc.* **2012**, *134*, 18510-18513.
- 156. X. Li, M. Banis, A. Lushington, X. Yang, Q. Sun, Y. Zhao, C. Liu, Q. Li, B. Wang, W. Xiao, C. Wang, M. Li, J. Liang, R. Li, Y. Hu, L. Goncharova, H. Zhang, T.K. Sham, X. Sun, Nat. Commun. 2018, 9, 4509.
- 157. S. Wei, L. Ma, K.E. Hendrickson, Z. Tu, L.A. Archer, *J. Am. Chem. Soc.* **2015**, *137*, 12143-12152.
- 158. J. Ma, G. Xu, Y. Li, C. Ge, X. Li, Chem. Commun. 2018, 54, 14093-14096.
- 159. S.S. Zhang, *J. Power Sources* **2013**, *231*, 153-162.
- 160. M. Li, Z.W. Chen, T.P. Wu, J. Lu, Adv. Mater. 2018, 30, 1801190.
- 161. Y.S. Su, A. Manthiram, *Nat. Commun.* **2012**, *3*, 1166.

- 162. R. Singhal, S.H. Chung, A. Manthiram, V. Kalra, J. Mater. Chem. A 2015, 3, 4530-4538.
- 163. Y.S. Su, A. Manthiram, Chem. Commun. 2012, 48, 8817-8819.
- 164. X. Liu, J.Q. Huang, Q. Zhang, L. Mai, Adv. Mater. 2017, 29, 1601759.
- 165. N. Ding, Y. Lum, S. Chen, S.W. Chien, T.S.A. Hor, Z. Liu, Y. Zong, J. Mater. Chem. A 2015, 3, 1853-1857.
- 166. Y. Shi, W. Lv, S. Niu, Y. He, G. Zhou, G. Chen, B. Li, Q.H. Yang, F. Kang, *Chem. Asian J.* **2016**, *11*, 1343-1347.
- 167. Z. Li, J. Zhang, B. Guan, D. Wang, L.M. Liu, X.W. Lou, Nat. Commun. 2016, 7, 13065.
- 168. J. Xu, H. Zhen, J. Wu, K. Song, J. Wu, H. Gao, Y.H. Mi, *Mater. Chem. Phys.* **2018**, *205*, 359-365.
- 169. Y. Wu, T. Momma, S. Ahn, T. Yokoshima, H. Nara, T. Osaka, *J. Power Sources* **2017**, *366*, 65-71.
- 170. F. Wu, E. Zhao, D. Gordon, Y. Xiao, C. Hu, G. Yushin, Adv. Mater 2016, 28, 6365-6371.
- 171. G. Zhou, E. Paek, G. Hwang, A. Manthiram, *Adv. Energy Mater.* **2016**, *6*, 1501355.
- 172. Y. Chen, S. Lu, J. Zhou, X. Wu, W. Qin, O. Ogoke, G. Wu, *J. Mater. Chem. A* **2017**, *5*, 102-112.
- 173. D.H. Wang, D. Xie, T. Yang, Y. Zhong, X.L. Wang, X.H. Xia, C.D. Gu, J.P. Tu, *J. Power Sources* **2016**, *331*, 475-480.
- 174. M.L. Yu, Z.Y. Wang, Y.W. Wang, Y.F. Dong, J.S. Qiu, *Adv. Energy Mater.* **2017**, *7*, 1700018.
- 175. S. Li, G. Ren, M.N.F. Hoque, Z. Dong, J. Warzywoda, Z.Y. Fan, *Appl. Surf. Sci.* **2017**, *396*, 637-643.
- 176. L. Yang, G. Li, X. Jiang, T. Zhang, H. Lin, J.Y. Lee, *J. Mater. Chem. A* **2017**, *5*, 12506-12512.
- 177. L.B. Xing, K. Xi, Q. Li, Z. Su, C. Lai, X. Zhao, R.V. Kumar, *J. Power Sources* **2016**, 303, 22-28.
- S. Zhang, M. Liu, F. Ma, F. Ye, H. Li, X. Zhang, Y. Hou, Y. Qiu, W. Li, J. Wang, J. Wang,
 Y. Zhang, J. Mater. Chem. A 2015, 3, 18913-18919.
- 179. V.C. Hoang, V. Do, I.W. Nah, C. Lee, W.I. Cho, I.H. Oh, *Electrochim. Acta* **2016**, *210*,

- 1-6.
- 180. X.B. Cheng, R. Zhang, C.Z. Zhao, Q. Zhang, Chem. Rev. 2017, 117, 10403-10473.
- 181. Q.C. Liu, J.J. Xu, S. Yuan, Z.W. Chang, D. Xu, Y.B. Yin, L. Li, H.X. Zhong, Y.S. Jiang, J.M. Yan, X.B. Zhang, Adv. Mater 2015, 27, 5241-5247.
- 182. F. Wu, H. Kim, A. Magasinski, J.T. Lee, H.T. Lin, G. Yushin, *Adv. Energy Mater.* **2014**, *4*, 1400196.
- 183. F. Wu, J.T. Lee, E. Zhao, B. Zhang, G. Yushin, ACS Nano 2016, 10, 1333-1340.
- 184. J. He, Y. Chen, W. Lv, K. Wen, P. Li, F. Qi, Z. Wang, W. Zhang, Y. Li, W. Qin, W. He, *J. Power Sources* **2016**, *327*, 474-480.
- 185. Y. Wu, T. Yokoshima, H. Nara, T. Momma, T. Osaka, *J. Power Sources* **2017**, *342*, 537-545.
- 186. Z. Li, Y. Kamei, M. Haruta, T. Takenaka, A. Tomita, T. Doi, S. Zhang, K. Dokko, M. Inaba, M. Watanabe, *Electrochemstry* **2016**, *84*, 887-890.
- 187. X. Xu, J. Cheng, Y. Li, X. Nie, L. Dai, L. Ci, J. Solid State Electr. 2019, 23, 3145-3151.
- 188. H. Jha, I. Buchberger, X.Y. Cui, S. Meini, H.A. Gasteiger, *J. Electrochem. Soc.* **2015**, *162*, 1829-1835.
- 189. J. Hassoun, B. Scrosati, *Angew. Chem. Int. Ed.* **2010**, 49, 2371-2374.
- 190. B. Wang, B. Luo, X.L. Li, L.J. Zhi, Mater. Today 2012, 15, 544-552.
- 191. Y. Jiang, Z.J. Jiang, L. Yang, S. Cheng, M. Liu, J. Mater. Chem. A 2015, 3, 11847-11856.
- 192. H. Wu, Y. Cui, *Nano Today* **2012**, *7*, 414-429.
- 193. R. Hu, Y. Ouyang, T. Liang, H. Wang, J. Liu, J. Chen, C. Yang, L. Yang, M. Zhu, *Adv. Mater.* **2017**, *29*, 1605006.
- 194. C.K. Chan, H. Peng, G. Liu, K. McIlwrath, X.F. Zhang, R.A. Huggins, Y. Cui, *Nat. Nanotechnol.* **2008**, *3*, 31-35.
- 195. D.P. Lv, P.F. Yan, Y.Y. Shao, Q.Y. Li, S. Ferrara, H.L. Pan, G.L. Graff, B. Polzin, C.M. Wang, J.G. Zhang, Chem. Commun. 2015, 51, 13454-13457.
- 196. T. Jaumann, J. Balach, M. Klose, S. Oswald, J. Eckert, L. Giebeler, *J. Electrochem. Soc.* **2016**, *163*, A557-A564.
- 197. A. Manthiram, X. Yu, S. Wang, *Nat. Rev. Mater.* **2017**, *2*, 16103.

- 198. X. Ban, W. Zhang, N. Chen, C. Sun, J. Mater. Chem. C 2018, 122, 9852-9858.
- 199. S.S. Zhang, *Electrochim. Acta* **2012**, *70*, 344-348.
- 200. S. Xiong, K. Xie, Y. Diao, X. Hong, J. Power Sources 2013, 236, 181-187.
- 201. H. Yang, Q. Li, C. Guo, A. Naveed, J. Yang, Y. Nuli, J. Wang, *Chem. Commun.* 2018, 54, 4132-4135.
- 202. H.L. Wu, M. Shin, Y.M. Liu, K.A. See, A.A. Gewirth, Nano Energy 2017, 32, 50-58.
- 203. D. Zhou, M. Liu, Q. Yun, X. Wang, Y.B. He, B. Li, Q.H. Yang, Q. Cai, F. Kang, *Small* 2017, 13, 1602015.
- 204. M. Liu, D. Zhou, H.R. Jiang, Y.X. Ren, F.Y. Kang, T.S. Zhao, *Nano Energy* **2016**, *28*, 97-105.

Declaration of interests

☐ The authors declare that they have no known competing financhat could have appeared to influence the work reported in this p	·
☐ The authors declare the following financial interests/personal reas potential competing interests:	elationships which may be considered